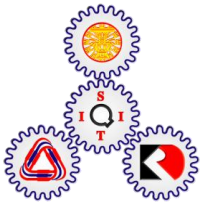

MICROWAVE GRAPHENE OXIDE: A NOVEL SORBENT FOR SLOW RELEASE OF AROMA COMPOUNDS

BY

NEUNGRUTHAI TIPPO

A THESIS SUBMITTED IN PARTIAL FULFILLMENT OF THE REQUIREMENTS FOR THE DEGREE OF MASTER OF ENGINEERING (ENGINEERING TECHNOLOGY)

SIRINDHORN INTERNATIONAL INSTITUTE OF TECHNOLOGY

THAMMASAT UNIVERSITY

ACADEMIC YEAR 2016

Ref. code: 25595722040614EIP

MICROWAVE GRAPHENE OXIDE: A NOVEL SORBENT FOR SLOW RELEASE OF AROMA COMPOUNDS

BY

NEUNGRUTHAI TIPPO

A THESIS SUBMITTED IN PARTIAL FULFILLMENT OF THE REQUIREMENTS FOR THE DEGREE OF MASTER OF ENGINEERING (ENGINEERING TECHNOLOGY)

SIRINDHORN INTERNATIONAL INSTITUTE OF TECHNOLOGY

THAMMASAT UNIVERSITY

ACADEMIC YEAR 2016

Ref. code: 25595722040614EIP

MICROWAVE GRAPHENE OXIDE: A NOVEL SORBENT FOR SLOW RELEASE OF AROMA COMPOUNDS

A Thesis presented

By

NEUNGRUTHAI TIPPO

Submitted to

Sirindhorn International Institute of Technology

Thammasat University

In partial fulfillment of the requirements for the degree of

MASTER OF ENGINEERING (ENGINEERING TECHNOLOGY)

Approved as to style and content by

Advisor and Chairperson of Thesis Committee _____

(Asst. Prof. Dr. Paiboon Sreearunothai)

Committee Member and
Chairperson of Examination Committee _____

(Assoc. Prof. Dr. Pakorn Opaprakasit)

Committee member _____

(Dr. Boonyawan Yoosuk)

Committee member _____

(Assoc. Prof. Dr. Ryuichi Egashira)

MAY 2017

Abstract

MICROWAVE GRAPHENE OXIDE: A NOVEL SORBENT FOR SLOW RELEASE OF AROMA COMPOUNDS

by

NEUNGRUTHAI TIPPO

Bachelor of Science (Environmental Science), Thammasat University, 2009

Master of Engineering (Engineering Technology), Sirindhorn International Institute of Technology, 2014

Aromatherapy products are in demand all over the world. A wide variety of products is made to meet this demand, such as air spray, candle, diffuser sheet, incense, perfume reed diffuser, potpourri, and scented gel. However, the scented lifetimes of those products are usually quite short. This work studies the use of microwave graphene oxide for use as a novel sorbent material for control release of aroma compounds, microwave graphene oxide (mGO). mGO can be easily synthesized using microwave at 700 watts within 1 minute which is a simple and rapid. Aroma compounds used in this work including menthol, thymol, citronellol, and geraniol were loaded into microwave graphene oxide. The release performance of the mGO was studied by the thermogravimetric analysis, the weights of the composites were monitored at the temperature of 80°C until all of the aroma compounds evaporated. When comparing the results of mGO with traditional essential oil reed diffuser and the pure aroma compounds, it was found that mGO can significantly slow down the menthol release rate compared to that of the pure menthol up to 8 times slower than the pure menthol. In addition, mGO can slow down the release rate of thymol and citronellol by about 3 and 4 times, respectively. Conversely, geraniol on mGO has a fast release rate compared to pure geraniol comparing to the pure substances around 3 times. The interaction of composites were also studied using Fourier transform infrared spectroscopy (FTIR) and ^{1}H-NMR which indicates that mGO changes the chemical structure of menthol and geraniol leading to the slow release of menthol and fast release of geraniol. While mGO has a few effect on the release rate of thymol and citronellol, as it is only physical absorption. The release rate of thymol and citronellol adsorbed on the mGO are not changed significantly.

Keywords: Reduced graphene oxide, Microwave graphene oxide, Essential oils, Menthol, Thymol, Citronellol, Geraniol, Slow release

Ref. code: 25595722040614EIP

Acknowledgements

The author gratefully acknowledges Thailand Advanced Institute of Science and Technology (TAIST-Tokyo Tech) and Sirindhorn International Institute of Technology (SIIT), Thammasat University for providing the scholarship. The author would like to thank Dr. Paiboon Sreearunothai at SIIT for his attention, his helpful, his suggestion, and his support. Dr. Pakorn Opaprakasit for the valuable suggestion and discussion of this results. In addition, special appreciation to Dr. Jedsada Manyum from NANOTEC, and Dr. Boonyawan Yoosuk from MTEC for their advice and their support with scientific instruments and equipments. And thanks to Dr. Egashira ryuichi for his careful and good opportunity in this program.

Ref. code: 25595722040614EIP

Table of contents

Chapter	Title	Page
	Signature page	i
	Abstract	ii
	Acknowledgements	iii
	Table of contents	iv
	List of figures	vii
	List of tables	xi
1	Introduction	1
	1.1 Concept and significance	1
	1.2 Objectives of the study	2
	1.3 Scope of study	2
2	Literature Review	3
	2.1 Aroma compounds	3
	2.1.1 L-Menthol	3
	2.1.2 Thymol	4
	2.1.3 Citronellol	4
	2.1.4 Geraniol	5
	2.2 Materials for controlled release of essential oils	6
	2.3 Graphite oxide, graphene oxide, and reduced graphene oxide	7
	2.4 Adsorption of aroma compounds into sorbents	9
3	Methodology	11
	3.1 Reagents and equipment	11
	3.2 Preparation of microwave graphene oxide (mGO)	11

Ref. code: 25595722040614EIP

3.3 Loading of menthol, thymol, citronellol, and geraniol 12
3.4 Characterizations 12
3.4.1 Laser confocal scanning microscope 12
3.4.2 Scanning electron microscope (SEM) 12
3.4.3 Thermogravimetric analysis (TGA) 12
3.4.4 Fourier transform infrared spectroscopy (FTIR) 12
3.4.5 Proton-nuclear magnetic resonance (^{1}H-NMR) 13
3.4.6 X-ray diffraction (XRD) 13
3.4.7 Differential scanning calorimetry (DSC) 13
3.4.8 Brunauer-emmett-teller (BET) 13

4 Results and Discussion 14

4.1 Physical appearance of the samples 14
4.2 The average release rate of the aroma compounds and thermogravimetric analysis 16
4.2.1 Menthol 17
4.2.2 Thymol 21
4.2.3 Citronellol 22
4.2.4 Geraniol 23
4.3 Loading efficiency and actual percent loading of aroma compounds 24
4.3.1 Menthol 24
4.3.2 Thymol 26
4.3.3 Citronellol 27
4.3.4 Geraniol 28
4.4 FTIR 30
4.4.1 Menthol 30
4.4.2 Thymol 33
4.4.3 Citronellol 35
4.4.4 Geraniol 36
4.5 ^{1}H-NMR 38

Ref. code: 25595722040614EIP

4.6 X-ray diffraction (XRD) 45
4.6.1 Menthol 45
4.6.2 Thymol 47
4.7 Differential scanning calorimetry (DSC) 47
4.8 Specific surface area 49

5 Conclusions and Recommendations 51

References 53

Ref. code: 25595722040614EIP

List of figures

Figures	Page
2.1 The structure of L-menthol	3
2.2 The structure of thymol	4
2.3 The structure of citronellol	5
2.4 The structure of geraniol	5
2.5 The structure of cellulose in reed diffuser	6
2.6 The system of graphite to reduced graphene oxide	7
2.7 The reduction of graphene oxide	8
2.8 The structure of reduced graphene oxide	8
2.9 A three dimensional rendering of prior art reed diffusers	9
3.1 Microwave graphene oxide (mGO)	11
3.2 Reed diffuser	12
4.1 Images of menthol (A-B), mGO (C), menthol-loaded mGO in the ratio of 1:0.5 (D), 1:1 (E), and 1:2 (F) from Confocal Laser Scanning Microscope at 10X.	15
4.2 Images of filter paper (A), menthol-loaded filter paper in the ratio of 1:1 (B), reed diffuser (C), menthol-loaded reed diffuser in the ratio of 1:1 (D) from Confocal Laser Scanning Microscope at 10X.	15
4.3 SEM images of (a) mGO, (b) filter paper, and (c) reed diffuser with a size of 50 μm.	16
4.4 The average release rate of (a) menthol, (b) menthol-loaded mGO in the ratio of 1:0.5, and (c) 1:1, (d) menthol-loaded filter paper in the ratio of 1:0.5, and (e) menthol-loaded reed diffuser in the ratio of 1:0.5 at temperature 80°C.	17
4.5 The average release rate of (a) menthol, (b) menthol-loaded mGO in the ratio of 1:0.5, and (c) 1:1 at temperature 30°C.	18
4.6 The average release rate of (a) menthol, (b) menthol-loaded mGO in the ratio of 1:0.5, and (c) 1:1 at temperature 60°C.	19
4.7 The average release rate of (a) menthol, (b) menthol-loaded mGO in the ratio of 1:0.5, and (c) 1:1 at temperature 100°C.	19

Ref. code: 25595722040614EIP

4.8 The temperature versus the average release rate of (a) menthol, (b) menthol-loaded mGO in the ratio of 1:0.5, and (c) 1:1. 20

4.9 The average release rate of (a) thymol, (b) thymol-loaded mGO in the ratio of 1:1, and (c) 1:2, (d) thymol-loaded filter paper in the ratio of 1:1 (d), and (e) thymol-loaded reed diffuser in the ratio of 1:1 at temperature 80°C. 21

4.10 The average release rate of (a) citronellol, (b) citronellol-loaded mGO in the ratio of 1:1, and (c) 1:2, (d) citronellol-loaded filter paper in the ratio of 1:1, and (e) citronellol-loaded reed diffuser in the ratio of 1:1 at temperature 80°C. 22

4.11 The average release rate of (a) geraniol, (b) geraniol-loaded mGO in the ratio of 1:1, and (c) 1:2, (d) geraniol-loaded filter paper in the ratio of 1:1, and (e) geraniol-loaded reed diffuser in the ratio of 1:1 at temperature 80°C. 23

4.12 The percent amount of menthol loaded of (a) menthol, (b) menthol-loaded mGO in the ratio of 1:0.5, and (c) 1:1, (d) menthol-loaded filter paper in the ratio of 1:0.5, and (e) menthol-loaded reed diffuser in the ratio of 1:0.5. The temperature were at 80℃. 25

4.13 The percent amount of (a) mGO, (b) filter paper, and (c) reed diffuser. The temperature were at 80℃. 25

4.14 The percent amount of thymol loaded of (a) thymol, (b) thymol-loaded mGO in the ratio of 1:1, and (c) 1:2, (d) thymol-loaded filter paper in the ratio of 1:1, and (e) thymol-loaded reed diffuser in the ratio of 1:1. The temperature were at 80℃. 26

4.15 The percent amount of citronellol loaded of (a) citronellol, (b) citronellol-loaded mGO in the ratio of 1:1, and (c) 1:2, (d) citronellol-loaded filter paper in the ratio of 1:1, and (e) citronellol-loaded reed diffuser in the ratio of 1:1. The temperature were at 80℃. 27

4.16 The percent amount of geraniol loaded of (a) geraniol, (b) geraniol-loaded mGO in the ratio of 1:1, and (c) 1:2, (d) geraniol-loaded filter paper in the ratio of 1:1, and (e) geraniol-loaded reed diffuser in the ratio of 1:1. The temperature were at 80℃. 28

4.17 The loading efficiency of menthol, thymol, citronellol, and geraniol. 30

4.18 FTIR spectra of (A) menthol-loaded mGO, (B) mGO, (C) menthol-loaded reed diffuser, (D) reed diffuser, (E) menthol-loaded filter paper, (F) filter paper, and (G) menthol at wavenumber 3600-600 cm^{-1}. 31

Ref. code: 25595722040614EIP

4.19 FTIR spectra of (a) menthol, and the subtraction spectra between the menthol-loaded sorbent and that of sorbent in order to show the FTIR spectra of the menthol on the sorbent of (b) menthol-loaded mGO, (c) menthol-loaded filter paper, and (d) menthol-loaded reed diffuser. A, B, C, D show the four different regions of the FTIR spectra at wavenumber 3400-2700 cm^{-1}, 1800-1650 cm^{-1}, 1050-900 cm^{-1}, and 750-600 cm^{-1}. 32

4.20 Reaction of menthol 33

4.21 Oxidation of menthol to menthone 33

4.22 FTIR spectra of (A) thymol-loaded mGO, (B) mGO, (C) thymol-loaded reed diffuser, (D) reed diffuser, (E) thymol-loaded filter paper, (F) filter paper, and (G) thymol at wavenumber 3600-600 cm^{-1}. 34

4.23 FTIR spectra of (a) thymol, and the subtraction spectra between the thymol-loaded sorbent and that of sorbent in order to show the FTIR spectra of the thymol on the sorbent of (b) thymol-loaded mGO, (c) thymol-loaded filter paper, and (d) thymol-loaded reed diffuser. A, B show the two different regions of the FTIR spectra at wavenumber 1500-1370 cm^{-1}, and 1280-1120 cm^{-1}. 34

4.24 FTIR spectra of (A) citronellol-loaded mGO, (B) mGO, (C) citronellol -loaded reed diffuser, (D) reed diffuser, (E) citronellol-loaded filter, (F) filter paper, and (G) citronellol at wavenumber 3600-600 cm^{-1}. 35

4.25 FTIR spectra of (a) citronellol, and the subtraction spectra between the citronellol-loaded sorbent and that of sorbent in order to show the FTIR spectra of the citronellol on the sorbent of (b) citronellol-loaded mGO, (c) citronellol-loaded filter paper, and (d) citronellol-loaded reed diffuser. A, B show the two different regions of the FTIR spectra at wavenumber 3000-2800 cm^{-1}, and 1080-960 cm^{-1}. 36

4.26 FTIR spectra of (A) geraniol-loaded mGO, (B) mGO, (C) geraniol-loaded reed diffuser, (D) reed diffuser, (E) geraniol-loaded filter paper, (F) filter paper, and (G) geraniol at wavenumber 3600-600 cm^{-1}. 37

4.27 FTIR spectra of (a) geraniol, and the subtraction spectra between the geraniol-loaded sorbent and that of sorbent in order to reveal the FTIR spectra of the geraniol on the sorbent of (b) geraniol-loaded mGO, (c) geraniol-loaded filter paper, and (d) geraniol-loaded reed diffuser. A, B show the two different regions of the FTIR spectra at wavenumber 3000-2750 cm^{-1}, and 1100-800 cm^{-1}. 37

4.28 Products of oxidation of geraniol 38

4.29 ^{1}H-NMR of mGO 39

Ref. code: 25595722040614EIP

4.30 ^{1}H-NMR of (A) menthol, and (B) menthol-loaded mGO 40

4.31 ^{1}H-NMR of (A) thymol, and (B) thymol-loaded mGO 41

4.32 ^{1}H-NMR of (A) citronellol, and (B) citronellol-loaded mGO 42

4.33 ^{1}H-NMR of (A) geraniol, and (B) geraniol-loaded mGO 43

4.34 ^{1}H-NMR of (A) reed diffuser, and (B) geraniol-loaded reed diffuser 44

4.35 XRD patterns of (A) mGO, (B) menthol-loaded mGO in the ratio of 1:1, (C) menthol-loaded mGO in the ratio of 1:2, (D) filter paper, (E) menthol-loaded filter paper in the ratio of 1:1, and (F) menthol at 5-30 degrees 2-theta. 45

4.36 Crystalline index (CI) of (A) menthol-loaded mGO in the ratio of 1:1, and (B) 1:2, and (C) menthol-loaded filter paper in the ratio of 1:1 at 7-25 degrees 2-theta from fityk program. 46

4.37 XRD patterns of (A) mGO, (B) thymol-loaded mGO in the ratio of 1:1, and (C) 1:2, (D) filter paper, (E) thymol-loaded filter paper in the ratio of 1:1, and (F) thymol. 47

4.38 DSC curves of menthol 48

4.39 DSC curves of thymol 48

4.40 BET-plot of mGO 49

4.41 BET-plot of filter paper 50

4.42 BET-plot of reed diffuser 50

Ref. code: 25595722040614EIP

List of tables

Tables	Page
2.1 The properties of aroma compounds.	6
4.1 Actual loading ratio of all composites.	29
4.2 Loading efficiency of aroma compounds on each sorbents.	29
4.3 Crystalline index (CI) of the menthol-loaded mGO in the ratio of 1:1, and 1:2, menthol-loaded filter paper in the ratio of 1:1.	46

Ref. code: 25595722040614EIP

Chapter 1

Introduction

1.1 Concept and significance

Smell has an influence on human life, so fragrance has been used widely in various types of products such as fabric softener, air freshener, cosmetic, medicine, food, and perfume. Smell plays an important role in all products for livelihood, especially air freshener products and fragrance diffuser products, such as air spray, ultrasonic aroma diffuser, diffuser sheet, perfume reed diffuser, aroma lamp, aroma burner, potpourri, candle, incense, and scented gel. Properties of essential oils include anticancer, anti-inflammatory, anti-nociceptive, antioxidative, antiviral, insects repellant, and penetration-enchancing [1]. It can be seen that the fragrance products have developed to meet the needs of consumers but one of the major problems in this product is the short lifespan. For this reason, it is necessary to improve the lifetime of products.

Currently, there are a variety of absorbent materials, one of them is the reduced graphene oxide. Reduced graphene oxide is the reduction of graphene oxide, prepared by chemical, thermal, or electrochemical. Graphene oxide (GO) is a material that is known and used for various applications. In the past, the synthesis of reduced graphene oxide is hazard and toxic. But nowadays, Zhu Y. et al. report a simple yet versatile method to simultaneously achieve the reduction of graphite oxide, reduced graphene oxide materials which could be synthesized by microwave oven [2]. Materials from the preparation of reduced graphene oxide by microwave oven are called microwave graphene oxide or “mGO”. The properties of mGO is a black fluffy, light weight, odorless, and high surface area. The absorption mechanisms of reduced graphene oxide are interesting to use as sorbent that may also act as control release of some aroma compounds.

The study aims to develop absorbent material based on mGO, which may be able to help control the release rate of aroma compounds including menthol (mint odor), thymol (thyme odor), citronellol (lemongrass odor), and geraniol (rose odor). Properties of the developed aroma compound-loaded mGO such as morphology, specific surface area, release rate, percent loading, loading efficiency, and interaction will also be studied and characterized.

Ref. code: 25595722040614EIP

1.2 Objectives of the study

This study has been developed to use reduced graphene oxide as a sorbent material. Significant parameters of the materials are then studied. The aims of this study are as follows;

(1) To synthesize reduced graphene oxide using the microwave technique and to characterize its morphology and structure.
(2) To determine the ability to absorb and release aroma compounds of the synthesized reduced graphene oxide.
(3) To compare the released rate of aroma compounds such as menthol, thymol, citronellol, and geraniol from the composites of mGO and aroma compounds with the composites of other conventional sorbent materials and aroma compounds, such as filter paper, and reed diffuser.

1.3 Scope of study

This study focuses on sorbent materials like reduced graphene oxide which be synthesized by microwave method, and natural sorbent materials such as filter paper and reed diffuser. For aroma compounds which be used in this study are such as menthol, thymol, citronellol, and geraniol. The release rate of aroma compounds from sorbent materials will be revealed by TGA.

Ref. code: 25595722040614EIP

Chapter 2

Literature review

This literature review shows about nature and properties of sorbent materials and aroma compounds which be used in this study. Microwave graphene oxide is one types of reduced graphene oxide which is synthesized by microwave thermal method. This includes how to synthesize and characterize them.

2.1 Aroma compounds

Aroma compounds or essential oils are chemical compounds that can evaporate easily and cause odor by reacting with human's olfactory. Aroma compounds can be found in perfume, fragrant oil, cosmetic, and food. Essential oils are widely used to prevent and treat human disease, cancer, cardiovascular disease including atherosclerosis and thrombosis, along with their bioactivity as antibacterial, antiviral antioxidants, and antidiabetic agents as well as natural skin penetration enhancers for transdermal drug delivery and therapeutic properties in aroma and massage therapy [3]. Aroma compounds which be used in this study are such as menthol, thymol, citronellol, and geraniol.

2.1.1 L-Menthol

L-Menthol is an alcohol produced from mint oils or prepared synthetically. Menthol is a white crystalline solid with a peppermint odor and taste. Molecular formula of menthol is $C_{10}H_{20}O$, and molecular weight is 156.27 g/mol. Boiling point is 212℃, and melting point is 41-43℃. It is very soluble in alcohol, chloroform, and ether. Menthol use as odor agents in cleaning and furnishing care products, food packaging, laundry and dishwashing products, personal care products, and water treatment products. Menthol's ability to chemically trigger cold-sensitive receptors in the skin is responsible for the well-known cooling sensation that it provokes when inhalated, eaten, or applied to the skin. Menthol is used to treat occasional minor irritation, pain, sore mouth, and sore throat as well as cough associated with a cold or inhaled irritants. It should be noted that menthol does not cause an actual drop in temperature [4].

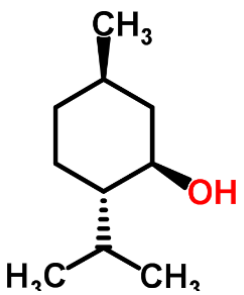

Figure 2.1 The structure of L-menthol [5].

Ref. code: 25595722040614EIP

Menthol is the one of popular aroma compounds that is widely used in food product, pharmaceutical, and cosmetics. Menthol is an isomer of monocyclic terpene, it has unique fragrance and cooling effect. Menthol can be added to skin-contact drug and cosmetics such as lotion and toothpaste. However, high volatility of menthol causes significant loss of menthol especially in applications where it is desirable to have slow but constant release of menthol over time such as in air freshener, or aroma freshener products [6]. Menthol is antioxidant activity, natural enhancers to improve the skin penetration and skin permeation of hydrophilic drugs [3, 7].

2.1.2 Thymol

Thymol is a phenol gained from thyme oil or other volatile oils. It is a pellets large crystals, colorless, translucent crystals or plates. Thymol has an odor of thyme, it looks like a spicy-herbal. Molecular formula of menthol is $C_{10}H_{14}O$, and molecular weight is 150.22 g/mol. Boiling point is 233℃, and melting point is 51℃. The use of thymol is a stabilizer in pharmaceutical preparations, and an antiseptic (antibacterial or antifungal) agent. It was formerly uses as an anthelmintic medicine. There are reports about properties of thymol as effective antioxidant [3, 8], anticancer, reduction of viral infectivity [3, 9], inhibition of the growth of bacterial [10], enhancing the skin penetration of labetalol hydrochloride (labetalol hydrochloride is used in the treatment of hypertension) and other constituent of drug [1, 7]. KK. Kuorwel shows that thymol can used as antimicrobial agents in active packaging films [11, 12]. Moreover, thymol can be used to kill bacteria in juice [13].

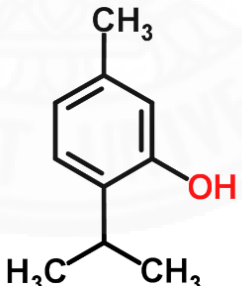

Figure 2.2 The structure of thymol [14].

2.1.3 Citronellol

Citronellol is a chemical compound that can be prepared by hydrogenation of geraniol. It is a colorless oily liquid at room temperature and provides lemongrass or fresh rosy odor. Molecular formula of citronellol is $C_{10}H_{20}O$ same as L-menthol. Molecular weight is 156.2652 g/mol. Boiling point is 224℃, and melting point is <-20℃. It is soluble in water, fixed oil, and propylene glycol. Citronellol is used as odor

Ref. code: 25595722040614EIP

agents in air care products, cleaning and furnishing care products, laundry and dishwashing products, and personal care products [15]. The important properties of citronellol is mosquito repellant. Citronellol possess a strong radical scavenging activity against the DPPH radical and is the component of anti-inflammatory medicine [1]. Furthermore, the rose oil containing citronellol and geraniol enhances the effectiveness of several antibiotics [16].

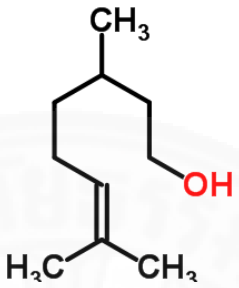

Figure 2.3 The structure of citronellol [17].

2.1.4 Geraniol

Geraniol is a chemical compound. It is colorless to pale yellow oily liquid with a sweet rose odor. Molecular formula of geraniol is $C_{10}H_{18}O$ and molecular weight is 154.25 g/mol. Boiling point is 230℃, and melting point is -15℃. The solubility of geraniol is in alcohol, ether, mineral oil, fixed oil, insoluble in water and glycerol. Geraniol is used as odor agents in cleaning and furnishing care products, laundry and dishwashing products, and personal care products [18]. There are reports about properties of geraniol are to enhance the skin penetration of labetalol hydrochloride, a strong antifungal potency, antibacterial, and antibiofilms activity [10]. De Souza EL et al. show the inhibitory effects of geraniol on bacteria in juice [13]. Moreover, geraniol candles caused a reduction of female mosquitoes by 82% and sand flies by 70%, it against mosquito and sand fly bites [1].

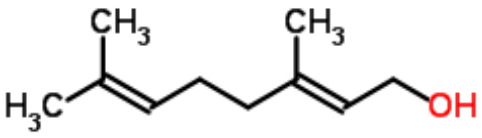

Figure 2.4 The structure of geraniol [19].

Ref. code: 25595722040614EIP

Table 2.1 The properties of aroma compounds.

	Menthol	**Thymol**	**Citronellol**	**Geraniol**
Structure	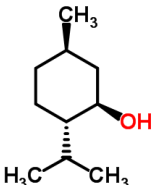	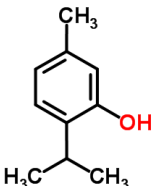	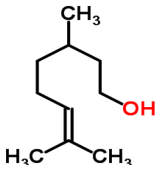	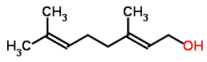
Formula	$C_{10}H_{20}O$	$C_{10}H_{14}O$	$C_{10}H_{20}O$	$C_{10}H_{18}O$
Color	Clear or white	Colorless	Colorless	Colorless to pale yellow
Status	Crystalline solid	Translucent crystals	Oily liquid	Oily liquid
Odor	Peppermint	Thyme	Lemongrass	Sweet rose
Melting point	41-43 °C	49-51 °C	<-20 °C	-15 °C
Boiling point	212 °C	233°C	224 °C	230 °C
Applications	- dental care - pharmacy - cosmetic - food flavor - fragrant	- stabilizer in pharmaceutical preparations - antiseptic agents - vermifuges	- odor agents - mosquito repellant - anti-inflammatory - antibiotics	- odor agents - mosquito repellant - antifungal - antibacterial - antibiofilms

2.2 Materials for controlled release of essential oils

Traditional aroma diffusers are such as air spray, ultrasonic aroma diffuser, diffuser sheet, perfume reed diffuser, aroma lamp, aroma burner, potpourri, candle, incense, and scented gel. Due to a short lifespan and an extremely low surface area of traditional products, novel materials for absorbed and controlled release of essential oils have been developed whether as-synthesized mesoporous silica [20], beeswax [21], cotton fabric [22], and zeolite X [23].

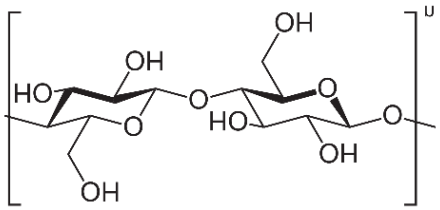

Figure 2.5 The structure of cellulose in reed diffuser.

Ref. code: 25595722040614EIP

2.3 Graphite oxide, graphene oxide, and reduced graphene oxide

Graphite oxide

Graphite oxide is the compound of carbon, hydrogen, and oxygen molecules. It obtains from treating graphite with strong oxidizers such as sulfuric acid. Oxidizers work by reacting with the graphite and removing an electron in the chemical reaction. Graphite oxide is often synthesized using the Hummers' method, in which graphite is treated by a mixture of sulfuric acid, sodium nitrate, and potassium permanganate.

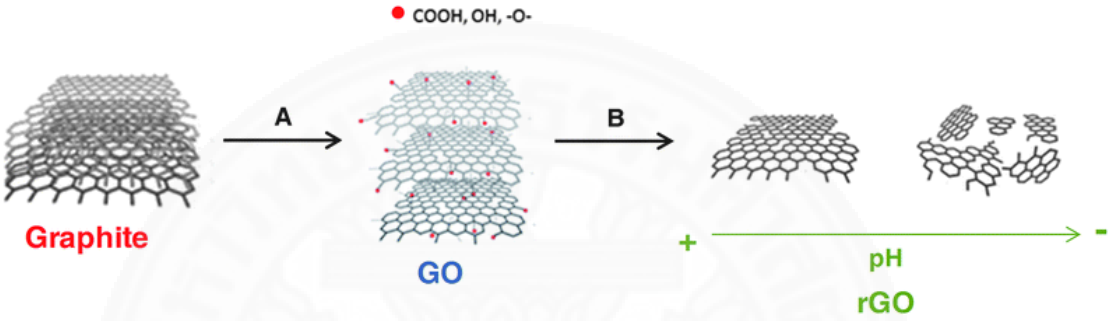

Figure 2.6 The system of graphite to reduced graphene oxide [24].

Graphene oxide

Graphene oxide is the by-product from the reaction of oxidizing agents with graphite. The interplanar spacing between the layers of graphite is increased. Graphene oxide is produced from dispersing of the completely oxidized compound dispersed in a base solution such as water. Chemical of graphite oxide and graphene oxide are similar, but the structure of both are different. The interplanar spacing between layers of the graphene oxide compounds is increased, caused by water intercalation and oxidization process [25]. The most popular method to synthesize graphene oxide is Hummers' method [26].

Experiment procedures for Hummers' method started from added concentrated H_2SO_4 (69 mL) to the mixture of graphite flakes (3 g.) and $NaNO_3$ (1.5 g.), and cooled the mixture to 0℃. Then, slowly added $KMnO_4$ (9 g.) in portions to keep the reaction temperature below 20℃. Warmed the reaction to 35℃ and stirred for 30 min, at which time slowly added water (138 mL), producing a large exotherm to 98℃. Maintained the temperature at 98℃ for 15 min, then removed the heat and cooled the reaction using a water bath for 10 min. Finally, added water (420 mL) and 30% H_2O_2 (3 mL). After air cooling, the mixture was purified by multiple washings, centrifugations and decanting, vacuum drying.

Reduced graphene oxide

The reduction of graphene oxide is reduced graphene oxide. There are many methods to prepare reduced graphene oxide based on chemical, thermal, or

Ref. code: 25595722040614EIP

electrochemical. Reduced graphene oxide (rGO) has created from graphene oxide (GO) by using chemical reduction. The obtain rGO from conventional method is low surface area and poor electronic conductibility. Although, reduced graphene oxide produced by thermal method in furnace at temperatures of 1000℃ or more has a very high surface area, but the heating process destroys the structure of graphene when the pressure increases and carbon dioxide is released [27].

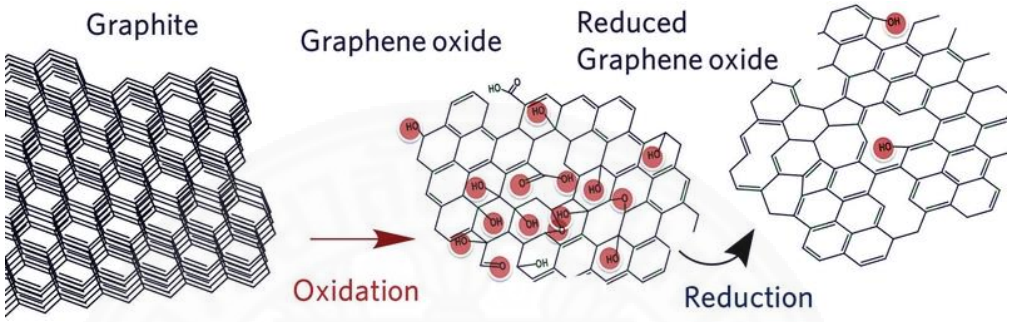

Figure 2.7 The reduction of graphene oxide [28].

One of the methods to create reducing graphene oxide is the use of microwave irradiation. Wei, T. et al. reports about rapid and efficient preparation to exfoliated graphite by microwave irradiation in a short time [29]. The mixtures can placed into a domestic microwave oven and irradiated at 700 W for 60 s. Microwave irradiation can be performed at room temperature in just 60 seconds which consumes less energy. Moreover, Zhu, Y., et al. reports a simple method to get the exfoliation and reduction of graphite oxide by treating graphite oxide powders in microwave oven, reduced graphene oxide materials can obtained within 1 min. Extensive characterizations indicated that prepared materials consisted of crumpled, few-layer thick and electronically conductive graphitic sheets [2].

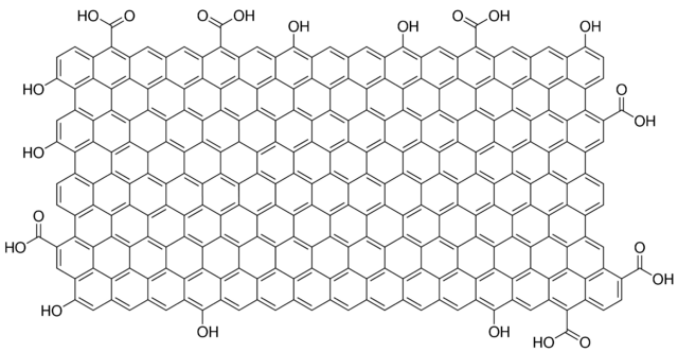

Figure 2.8 The structure of reduced graphene oxide [30].

Ref. code: 25595722040614EIP

2.4 Adsorption of aroma compounds into sorbents

Reed diffusers are widely used as common natural diffuser sorbent which deliver aroma oil to the atmosphere through the process of adsorption and desorption. Liquid composition of fragrance oils will be delivered through a wick which consists of many pores. The lower portions of the reeds absorb the fragrance oil and transport to the upper portions through capillary action. In this way, the entire length of the reed is saturated with fragrance oil, and the fragrance molecules desorb from the reeds and diffuse into the surrounding ambient atmosphere [31-33].

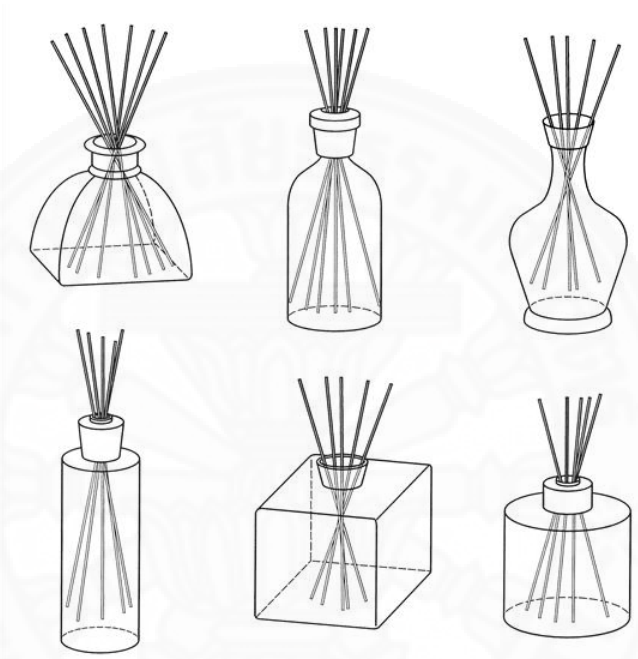

Figure 2.9 A three dimensional rendering of prior art reed diffusers [34].

For effective capillary action, wicks typically are set as a cord of fibers, such as cotton or fiberglass threads, braided in a rope-like configuration. In addition, the release of fragrance in traditional lamps is tied to the wick's ability to conduct heat to the reservoir of scented oil. However, materials that promote capillary action, i.e., porous material, often are poor heat conductors. Thus, the release of fragrance is not optimal. To combat this, wicks often are provided with materials having a high heat conductivity, such as copper wiring, compromising capillary action. Suitable capillary tubes that can be employed as a fluid transfer means can be constructed of glass, metal, plastic, or any other materials that are compatible with the liquid fuel and volatile material and that will allow the movement of the liquid by capillary action [35]. One of materials that have high heat conductivity and allow liquid movement is reduced graphene oxide.

Therefore, reed diffusers are not reusable and must be changed every time the scent is changed, or about once a month. The thin reeds or sticks that are used often become clogged up and must be thrown out.

Ref. code: 25595722040614EIP

Reduced graphene oxide foams possess the properties of hydrophobicity and superwetting behavior for organic solvents and good capillary action, an overall property that may be called selective superabsorbance, which makes rGO foams an excellent candidate for selective superabsorbance [36].

The interaction between liquid aroma compounds and the reduced graphene oxide is caused by capillary action. The organic solvents can disperse in the pores of the fiber wall of reduced graphene oxide by capillary forces. Reduced graphene oxide may acts as a sorbent [37].

The oil sorption capacity was the largest with the thinner micro-wrinkled reduced graphene oxide (MWrGO) due to the high surface area. The capillary rise of a liquid in the wrinkled structure of reduce graphene oxide can be described as:

$$h = \frac{2\gamma_{la}cos\theta}{d\rho g}$$

where h is the height that liquid can rise, γ_{la} is the surface tension of liquid, θ is the contact angle between liquid and rGO, d is distance between the wrinkles, ρ is the density of the liquid, and g is the constant of gravitational acceleration.

The low surface energy between oil and the inner wall of graphene drives the liquid oil towards the curvature space of wrinkles. This effect is related to the nature of the oleophilic rGO surface developed from the aromatic carbon rings of the rGO structure recovered during the chemical reduction process of graphene oxide, compatible with oil, which builts a directional interfacial force between oil and rGO. This phenomenon is very similar at the sub-micrometer scale of the graphene micro-waves to a capillary action in which h is position. Additionally, oil can be stored in the space generated by the wrinkled capillary structure, which endows the oil sorption ability to the rGO.

The oil uptake capacity is viscosity dependent as the higher the viscosity of the oils, the higher the sorption capacity. The graphene thickness was not found to have a significant impact on oil spreading rate and since sample rGO offered the highest oil sorption capacity. The oil capacity as a function of the exposure duration was fitted by a second-order sorption rate equation:

$$\frac{1}{Q_{max} - Q_t} - \frac{1}{Q_{max}} = kt$$

where t is the contacting time with oil, Q_{max} is the saturated sorption capacity, Q_t is the sorption capacity at time t, and k is the sorption constant.

The fitting results suggest that the fastest sorption rate is achieved in the oil with the lowest viscosity. The oil sorption capacity of MWrGO is higher than the traditional materials (e.g. activated carbon, straw, cotton, and wool fibres) and most of the polymer sponges (poly(lactic acid), polyurethane, polyester, and PDMS) and comparable to graphene or carbon nanotube based absorbers (aerogels, sponges and foams) [38].

Ref. code: 25595722040614EIP

Chapter 3

Methodology

3.1 Reagents and equipments

Graphite powder (99% min) was purchased from ACROS. Hydrochloric acid (HCl, LOBA, 35.4%), potassium permanganate ($KMnO_4$, UNIVAR, 99%), sodium nitrate ($NaNO_3$, LOBA, 99%), and sulfuric acid (H_2SO_4, Fisher Chemical, >95%, S.G. 1.83) were purchased from Apex Chemicals. Hydrogen peroxide (6% w/v) was bought from government pharmaceutical organization (GPO). The representative of aroma compounds used in this work are L-menthol (ACROS, 99.7%), thymol (ACROS, 99%), citronellol (ACROS, 95%), and geraniol (ACROS, 99%). Filter papers (Whatman™, No.4) and reed diffusers (from rattan plant) were used as reference sorbent materials for comparison.

3.2 Preparation of microwave graphene oxide (mGO)

The primary procedure in this preparation is the synthesis of graphene oxide by Hummers' method. In brief, 3 g. of graphite and 1.5 g of sodium nitrate were mixed with 23 ml of sulfuric acid in 1000 ml beaker (set in ice bath), slowly adding 9 g of potassium permanganate and heating to 35±3 ℃ for 30 minutes. After that, 138 ml of water was added and maintained at the temperature of 98 ℃ for 15 minutes. The last step, 420 ml of the water was added and 3 ml of hydrogen peroxide (30%) in order to stop the reaction. The obtained products were washed with 5%HCl and water two times, and then centrifuged at 4000 rpm for 5 minutes, and the dried in vacuum.

The second procedure is preparing the reduced graphene oxide using microwave heating (mGO). The obtained graphene oxide (GO) from the above procedure were treated by microwave irradiation at 700 watts for 1 minute. Microwave graphene oxide were then obtained after this preparation. The properties of mGO is black fluffy, light weight and odorless.

Figure 3.1 Microwave graphene oxide (mGO)

Ref. code: 25595722040614EIP

3.3 Loading of menthol, thymol, citronellol, and geraniol

In this experiment, menthol and thymol were added to mGO by providing heat and sonicated in ultrasonic bath at temperature 50℃ for 30 minutes. Filter paper, and reed diffuser were added with menthol or thymol as same as mGO for comparison. In this case, filter paper is representative of cellulose fiber, leaf, or flower. Dimension of reed diffuser and filter paper are around 2 x 2 mm (cut into small pieces ≈2x2 mm). For liquid aroma compounds, citronellol and geraniol were dropped onto sorbents including mGO, filter paper, and reed diffuser. After that, observed and characterized them.

Figure 3.2 Reed diffuser

3.4 Characterizations

3.4.1 Laser Confocal Scanning Microscope

The LEXT OLS4100 was used to reveal the surface morphology of menthol, sorbents, and menthol onto sorbents with 10X magnification.

3.4.2 Scanning Electron Microscope (SEM)

The surface morphology of mGO, filter paper, and reed diffuser were taken by scanning electron microscope (SEM, Hitachi S-3400N).

3.4.3 Thermogravimetric analysis (TGA)

Thermogravimetric analysis (TGA, Mettler Toledo TGA/SDTA851^{e}) was used to monitor weight loss of samples at constant temperature of 80°C until the weight loss became stabled. The condition of sample is under nitrogen gas at 30 mg/minute. The sample per time is around 5-15 mg which is fill in alumina crucible.

3.4.4 Fourier transform infrared spectroscopy (FTIR)

Chemical characteristics between sorbents and aroma compounds were analyzed by Fourier transform infrared spectroscopy (FTIR, NICOLET iS5). The attenuated total reflectance (ATR) mode using diamond head with deuterated, L-alanine doped triglycine (DTGS) detector (Thermo Scientific, Nicolet iS5 FT-IR). FTIR spectra were obtained after 32 scans from 4000 cm^{-1} to 525 cm^{-1}, with spectra resolution of 4 cm^{-1}.

Ref. code: 25595722040614EIP

3.4.5 Proton-Nuclear magnetic resonance (^{1}H-NMR)

Proton-Nuclear magnetic resonance (^{1}H-NMR, Bruker Avance-300 DPX) was used to reveal chemical structure of aroma compounds and sorbents. The solvents used in this experiment is d-chloroform ($CDCl_3$).

3.4.6 X-ray diffraction (XRD)

The entity of menthol and thymol on mGO were revealed by X-ray diffraction (XRD) at 5-40 degrees 2-theta.

3.4.7 Differential scanning calorimetry (DSC)

Differential scanning calorimetry (DSC, Mettler Toledo DSC823^e) was used to show melting point of menthol and thymol on sorbents. The weight of samples per time is around 1-2 mg which be packed in aluminum crucible.

3.4.8 Brunauer-Emmett-Teller (BET)

The specific surface area of mGO was revealed by BET (Belsorp max). The samples were pre-treat at 120°C for 6 hrs. Nitrogen gas was used to measure pore size and surface area of microwave graphene oxide.

Ref. code: 25595722040614EIP

Chapter 4

Results and Discussion

4.1 Physical appearance of the samples

The physical appearance of the samples after mixing mGO and menthol together at low loading of 1:0.5, and 1:1 appear to be homogeneous. In contrast, at higher menthol loading of 1:1.5 and 1:2, white crystals of menthol start to be observed. In addition, the filter paper, or reed diffuser, loaded with menthol in the ratio of 1:0.5 and higher ratios, they appear to be heterogeneous.

For thymol, all of mixed samples in the ratio of 1:1, and 1:2 are homogeneous. The crystal of thymol cannot be found and they seem to be wet at room temperature (≈27°C).

For the liquid aroma compounds such as citronellol and geraniol, the appearance of samples after mixing mGO with citronellol or geraniol together at all loading of 1:1, and 1:2 appear dry and homogeneous. The mixture of the filter paper with citronellol or geraniol in the ratio of 1:1 appears to be wet, which is same as reed diffuser. Filter papers and reed diffusers are so wet because they probably cannot load liquid aroma compounds so well.

The menthol scent can be smell in all of the menthol-loaded samples even at the smallest ratio of 1:0.5. The scent of thymol also can be smell in every samples. The citronellol and geraniol fragrance can be smell in all of samples.

Figure 4.1 shows images of the crystal of menthol, the black fluffy of mGO, and the menthol-loaded mGO in the ratio of 1:0.5, 1:1, and 1:2 from Confocal Laser Scanning Microscope. The crystal of menthol on mGO can be found only at high loading ratio of 1:2. These images support the heterogeneity of composites in the ratio of 1:2 and the homogeneity of menthol-loaded mGO in the ratio of 1:0.5 and 1:1. Menthol-loaded filter paper and menthol-loaded reed diffuser in Figure 4.2 presents crystals of menthol on surfaces, that is supported the heterogeneity of menthol and natural sorbent in the ratio of 1:1.

Surface morphology of the materials were revealed by SEM images. Overlapping flake sheets of mGO (a), filter paper (b), and reed diffuser (c) in size of 50 μm are shown in Figure 4.3. Surface morphology of mGO is a stack of many flake sheets while filter paper seems to be cellulose fiber with pore and reed diffuser similar to rod shape packed together.

Ref. code: 25595722040614EIP

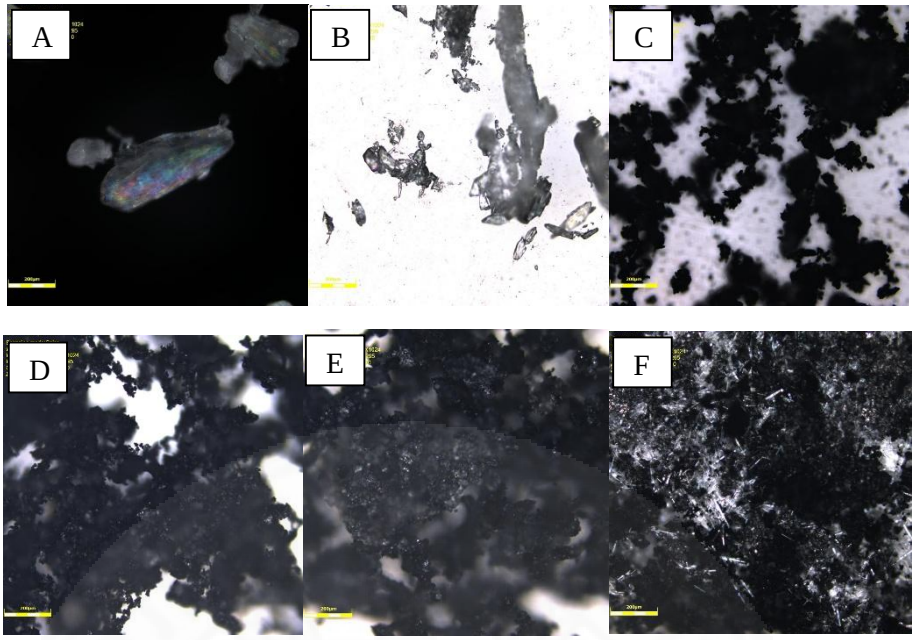

Figure 4.1 Images of menthol (A-B), mGO (C), menthol-loaded mGO in the ratio of 1:0.5 (D), 1:1 (E), and 1:2 (F) from Confocal Laser Scanning Microscope at 10X.

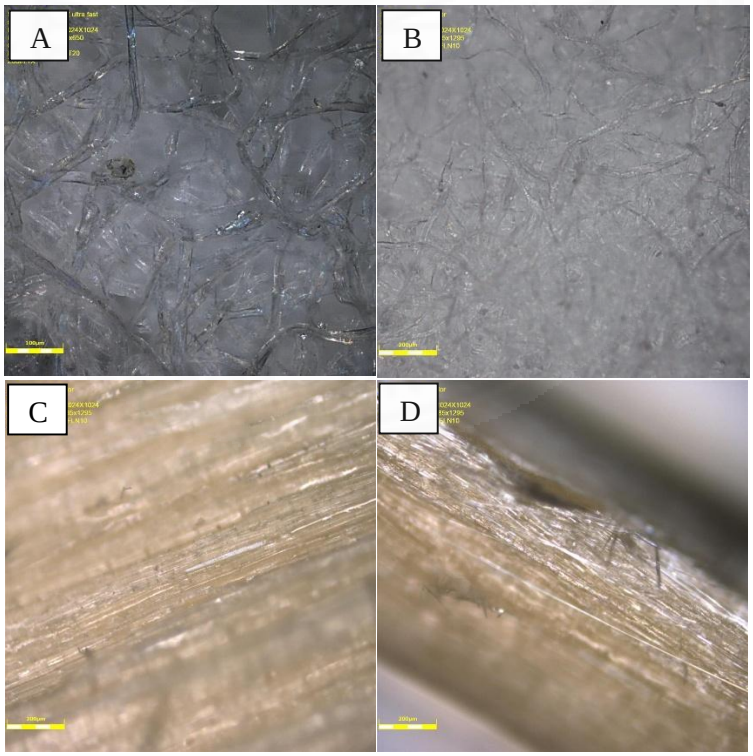

Figure 4.2 Images of filter paper (A), menthol-loaded filter paper in the ratio of 1:1 (B), reed diffuser (C), and menthol-loaded reed diffuser in the ratio of 1:1 (D) from Confocal Laser Scanning Microscope at 10X.

Ref. code: 25595722040614EIP

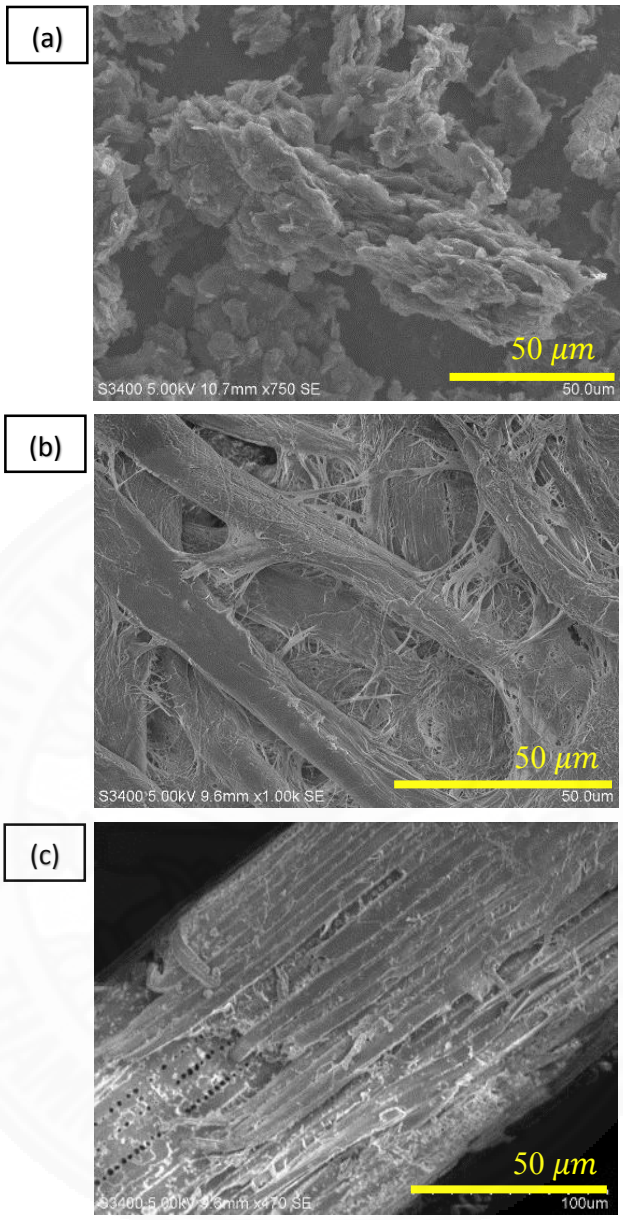

Figure 4.3 SEM images of (a) mGO, (b) filter paper, and (c) reed diffuser with a size of 50 μm.

4.2 The average release rate of the aroma compounds and thermogravimetric analysis

Thermogravimetric analysis (TGA) is used to measure sample's weight loss per minute while holding the composites at constant temperature. When all the aroma compounds have been released (by evaporation and sublimation) from the samples, the weight becomes constant and taken as the weight of the mGO substrate. From TGA curves of materials, average release rate (mg/minute) can be calculated.

Ref. code: 25595722040614EIP

$$\text{Average release rate} = \frac{Initial\ weight - Remaining\ weight\ (mg)}{Total\ time\ \ until\ stable\ weight\ (min)}$$

4.2.1 Menthol

The average release rate of menthol from TGA curves at several temperature of 30℃, 60℃, 80℃, and 100℃ can be shown in Fig. 4.4-4.7. Figure 4.4 shows the normalized weight loss of the samples as a function of time at a constant temperature of 80°C. The pure menthol weight constantly decreases as a function of time until all of the menthol completely evaporated at about 25 minutes. The menthol release rates from each substance are in the order from the fastest to the slowest as follows: 0.16 mg/min for pure menthol, 0.15 mg/min for filter paper:menthol (1:0.5), 0.13 mg/min for reed diffuser:menthol (1:0.5), 0.05 mg/min for mGO:menthol (1:1), and 0.02 mg/min for mGO:menthol (1:0.5). The menthol-loaded reed diffuser has a slightly faster rate of decrease initially, but the overall rate of decrease is slower than that of pure menthol. For comparison, filter paper and reed diffuser cannot decrease the release rate of menthol.

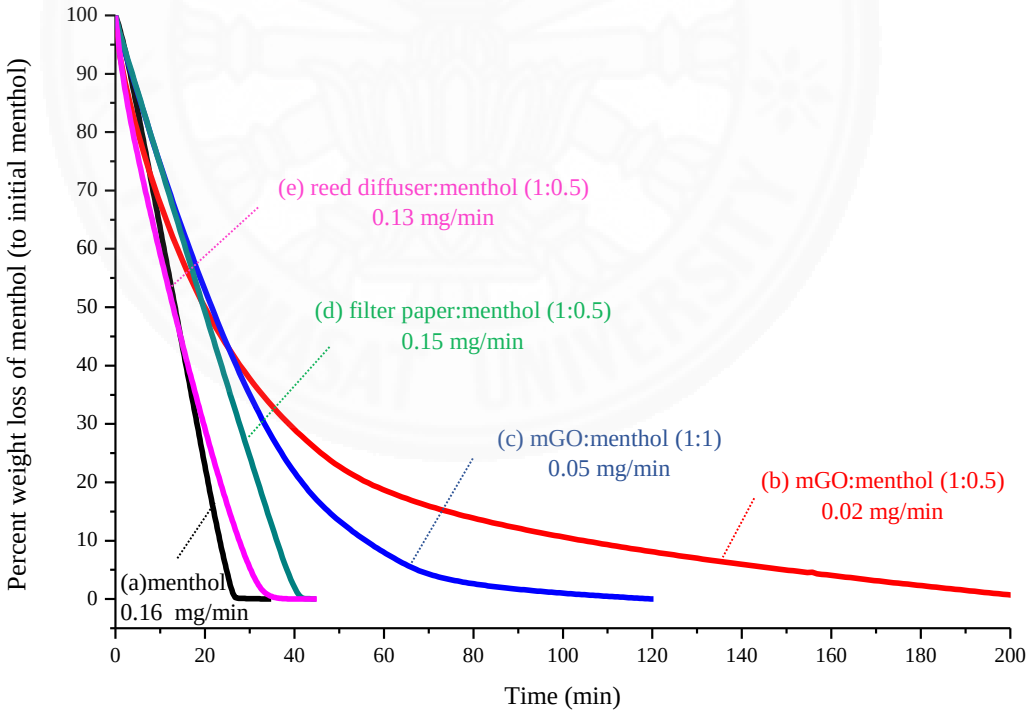

Figure 4.4 The average release rate of (a) menthol, (b) menthol-loaded mGO in the ratio of 1:0.5, and (c) 1:1, (d) menthol-loaded filter paper in the ratio of 1:0.5, and (e) menthol-loaded reed diffuser in the ratio of 1:0.5 at temperature **80°C**.

Ref. code: 25595722040614EIP

The 1:1 menthol-loaded mGO shows slower weight loss than those of pure menthol, reed diffuser or filter paper. Decreasing the menthol loading ratio from 1:1 to 1:0.5 decreases the rate even further. The rate of menthol release in menthol-loaded mGO at the 1:0.5 loading can be calculated to be about eight times slower than that of the pure menthol and seven times slower than that of traditional reed diffuser or filter paper. This indicates that mGO can help slow down the rate of menthol released from their structure compared to those of conventional sorbents. Therefore, mGO is a good material for slow release of menthol.

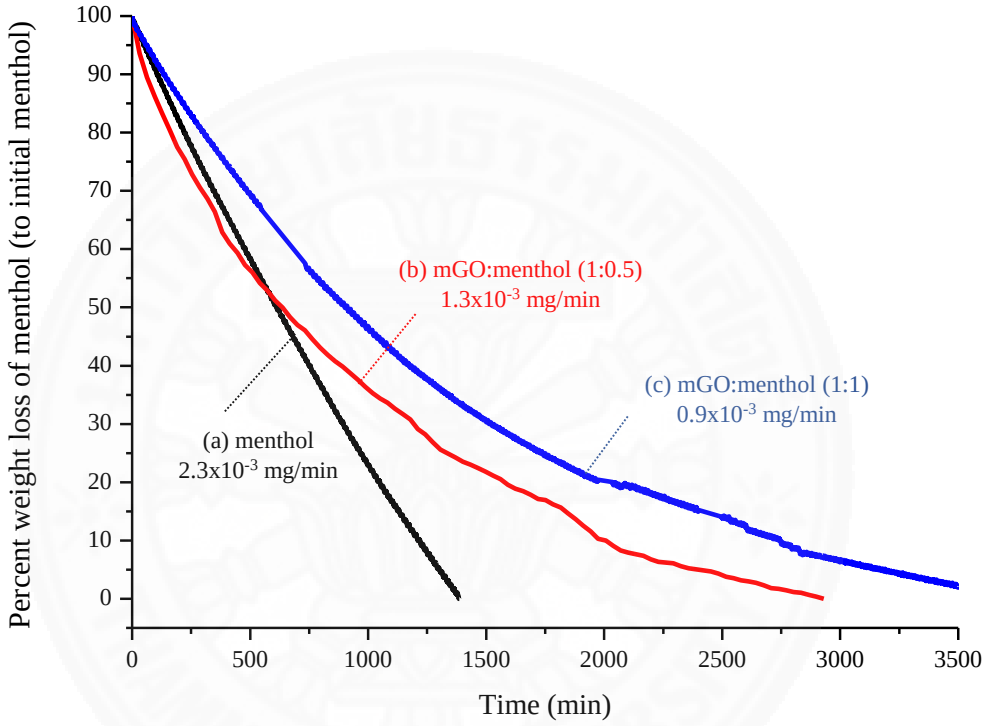

Figure 4.5 The average release rate of (a) menthol, (b) menthol-loaded mGO in the ratio of 1:0.5, and (c) 1:1 at temperature **30°C**.

Figure 4.5 shows the TGA curve while holding at constant temperature of 30°C. The curve of pure menthol has a constant rapid decay but the menthol-loaded mGO curves appear to decrease quite fast at first and very slow at later time when the menthol in the mGO is almost depleted. The release rate of pure menthol is calculated to be 2.3×10^{-3} mg/min while that of the menthol-loaded mGO do not have constant rate but their average release rates may be calculated to be 1.3×10^{-3} mg/min and 0.9×10^{-3} mg/min for the menthol loading ratio of 1:0.5 and 1:1, respectively. That means mGO can decrease the rate of menthol released by about 2 times.

Ref. code: 25595722040614EIP

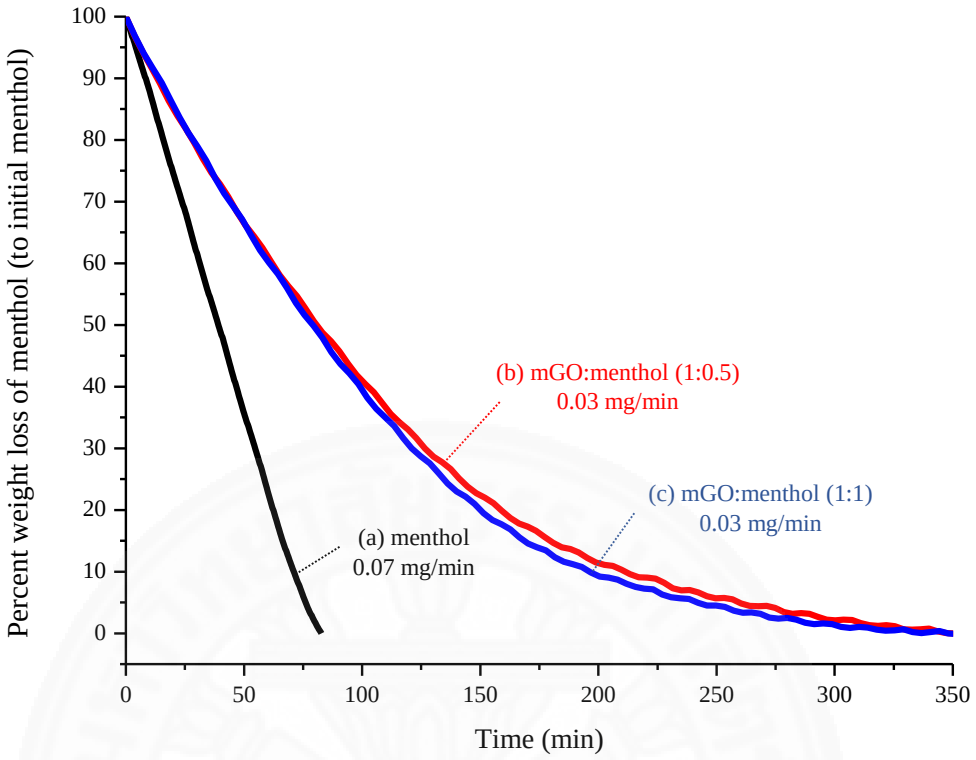

Figure 4.6 The average release rate of (a) menthol, (b) menthol-loaded mGO in the ratio of 1:0.5, and (c) 1:1 at temperature **60°C**.

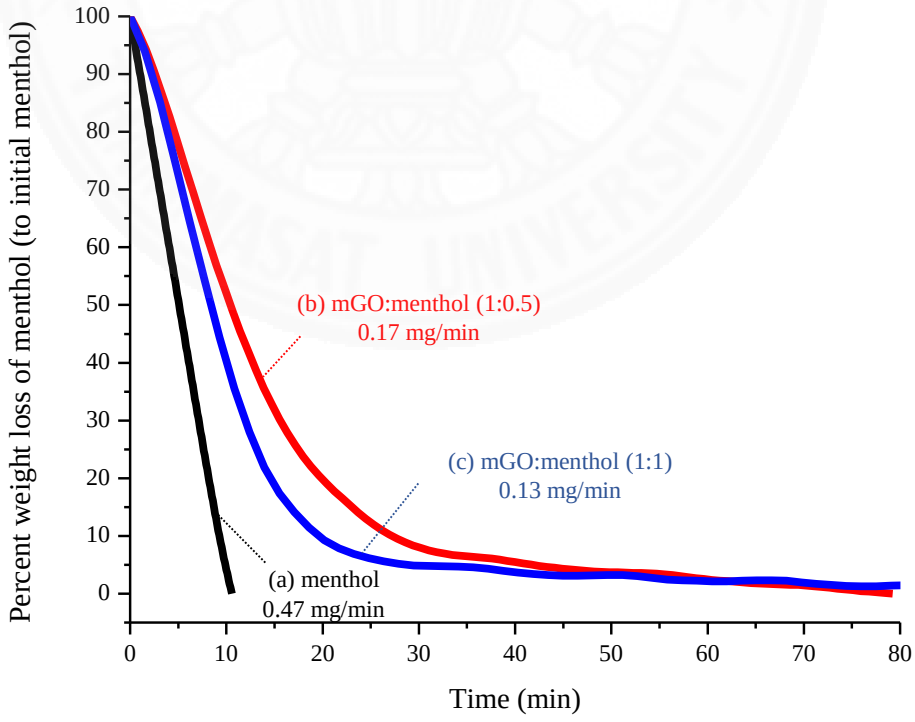

Figure 4.7 The average release rate of (a) menthol, (b) menthol-loaded mGO in the ratio of 1:0.5, and (c) 1:1 at temperature **100°C**.

Ref. code: 25595722040614EIP

The results at 60°C, and 100°C are similar to the results at 30°C except that the time to reach stable weight is much shorter resulting in faster release rates at higher temperatures. Figure 4.6 shows the release rate of pure menthol at 0.07 mg/min. The menthol-loaded mGO in the ratio of 1:0.5 is 0.03 mg/min, similar to the ratio of 1:1. mGO can decrease the release rate of menthol by about 2.3 times at temperature of 60°C. At temperature of 100°C (Figure 4.7), the release rate of pure menthol is 0.47 mg/min. For menthol-loaded mGO, the release rate is 0.17 mg/min for the 1:0.5 preparation ratio, and 0.13 mg/min for the 1:1 ratio (mGO:menthol). The release rate of menthol on mGO at temperature of 100°C decreases by about 3 times.

Figure 4.8 shows the trend of the average release rate at the several temperature of 30°C, 60°C, 80°C, and 100°C. The curves of menthol, menthol-loaded mGO in the ratio of 1:0.5, and 1:1 are exponential curve. These curves show that the higher the temperature is, the faster the average release rate will increase. Form this curves, menthol may be faster release than menthol-loaded mGO at higher temperature.

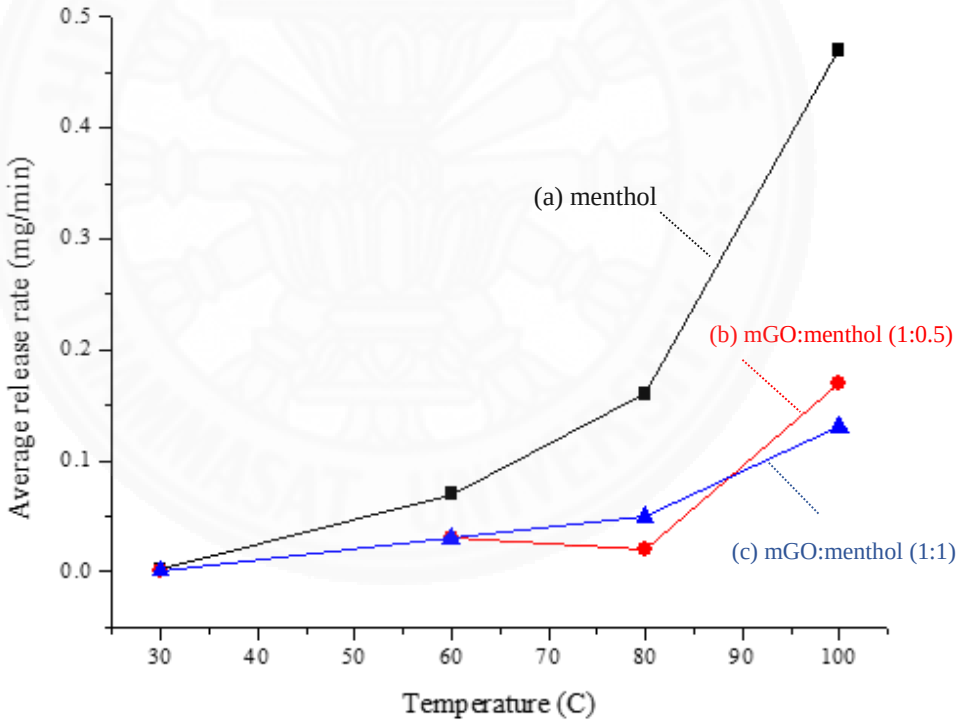

Figure 4.8 The temperature versus the average release rate of (a) menthol, (b) menthol-loaded mGO in the ratio of 1:0.5, and (c) 1:1.

Ref. code: 25595722040614EIP

4.2.2 Thymol

For another solid aroma compound like thymol, the percent weight loss of thymol and thymol onto sorbents at constant temperature of 80°C are shown in Figure 4.9.

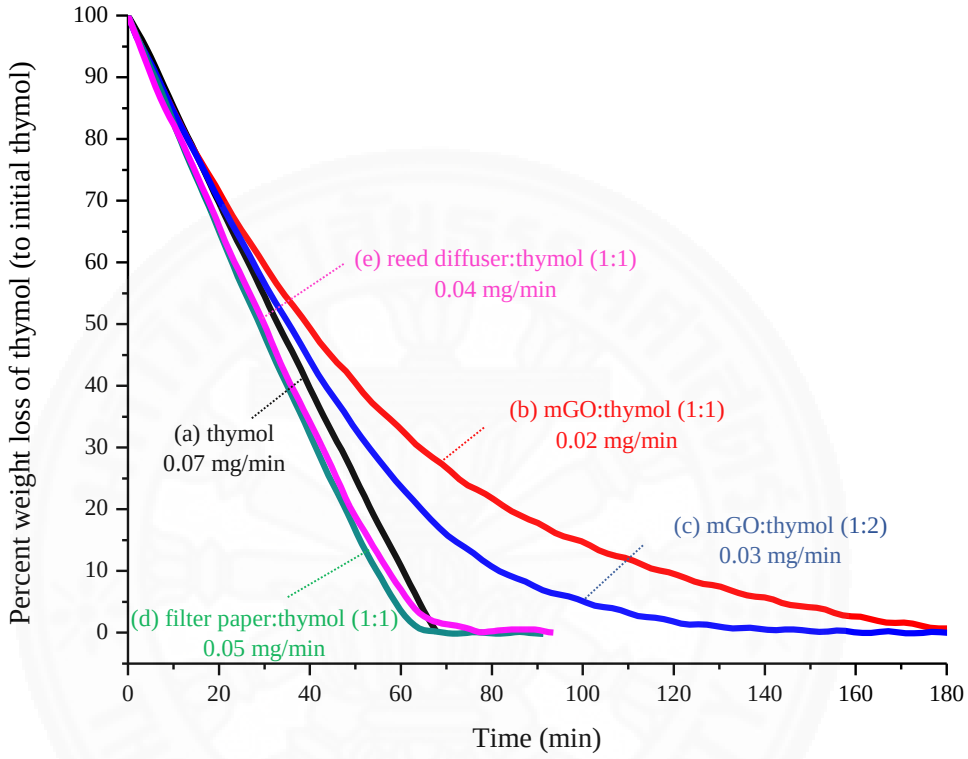

Figure 4.9 The average release rate of (a) thymol, (b) thymol-loaded mGO in the ratio of 1:1, and (c) 1:2, (d) thymol-loaded filter paper in the ratio of 1:1, and (e) thymol-loaded reed diffuser in the ratio of 1:1 at temperature **80°C**.

From Figure 4.9, the average release rate of thymol is 0.07 mg/min, the average rate of release for thymol-loaded mGO in the ratio of 1:1 and 1:2 are 0.02 mg/min and 0.03 mg/min, respectively. For thymol loaded on filter paper and reed diffuser, the average release rate are 0.05 mg/min and 0.04 mg/min, respectively. This result shows that, for thymol, common cellulosic sorbents like filter paper and reed diffuser cannot slow down the release rate of the thymol while mGO can slow down the average release rate compared to that of pure thymol by about 3 times slower.

Ref. code: 25595722040614EIP

4.2.3 Citronellol

For citronellol, which is in the liquid state at room temeperature, the percent weight loss of only the citronellol component can be shown in Figure 4.10. The overall release rates of citronellol-loaded sorbents are slower than that of pure citronellol.

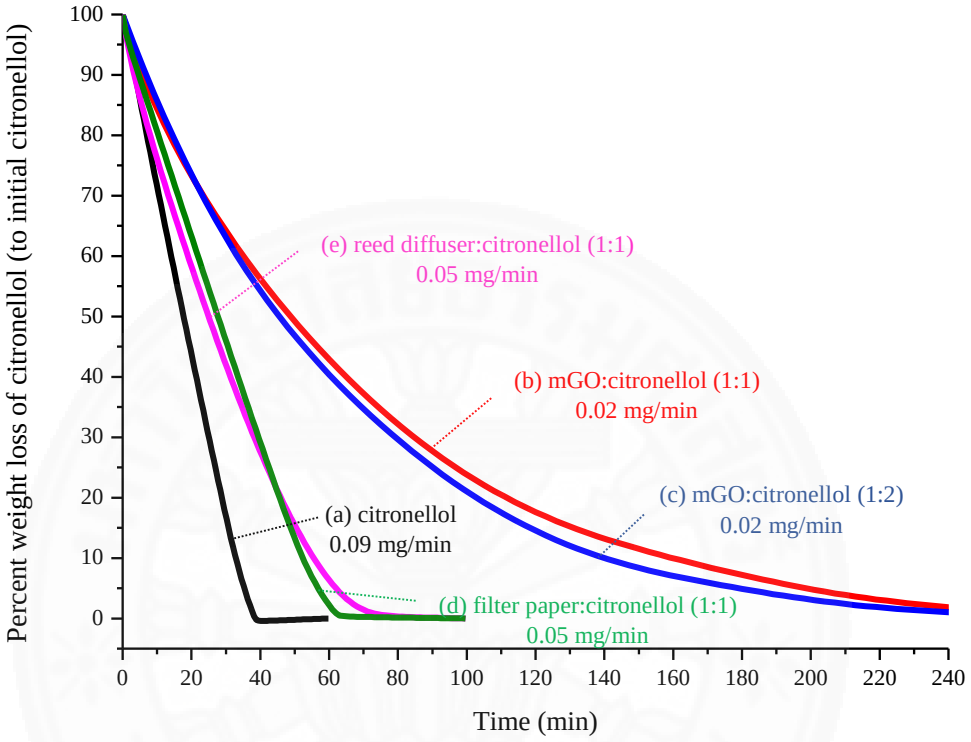

Figure 4.10 The average release rate of (a) citronellol, (b) citronellol-loaded mGO in the ratio of 1:1, and (c) 1:2, (d) citronellol-loaded filter paper in the ratio of 1:1, and (e) citronellol-loaded reed diffuser in the ratio of 1:1 at temperature **80°C**.

The citronellol-loaded mGO shows slower citronellol weight loss compared to that of the pure citronellol and citronellol-loaded filter paper and reed diffuser. The average release rate of pure citronellol is 0.09 mg/min. For citronellol-loaded mGO in the ratio of 1:1 and 1:2, their release rates are quite similar at around 0.02 mg/min while the release rate of filter paper and reed diffuser in the ratio of 1:1 are also similar at about 0.05 mg/min. This results show that citronellol in pure phase has the fastest release rate, while the citronellol-loaded onto mGO has the slowest release rate. The mGO can decreased the release rate of citronellol by about 4.5 times. Filter paper and reed diffuser can decrease the release rate of citronellol by about 1.8 times.

Ref. code: 25595722040614EIP

4.2.4 Geraniol

The percent weight loss of geraniol, which is the liquid aroma compound at room tempareture, can be shown in Figure 4.11. The release rate of geraniol on mGO is different from other aroma compounds on mGO. The geraniol-loaed mGO in the ratio of 1:1 and 1:2 are fastest release rate.

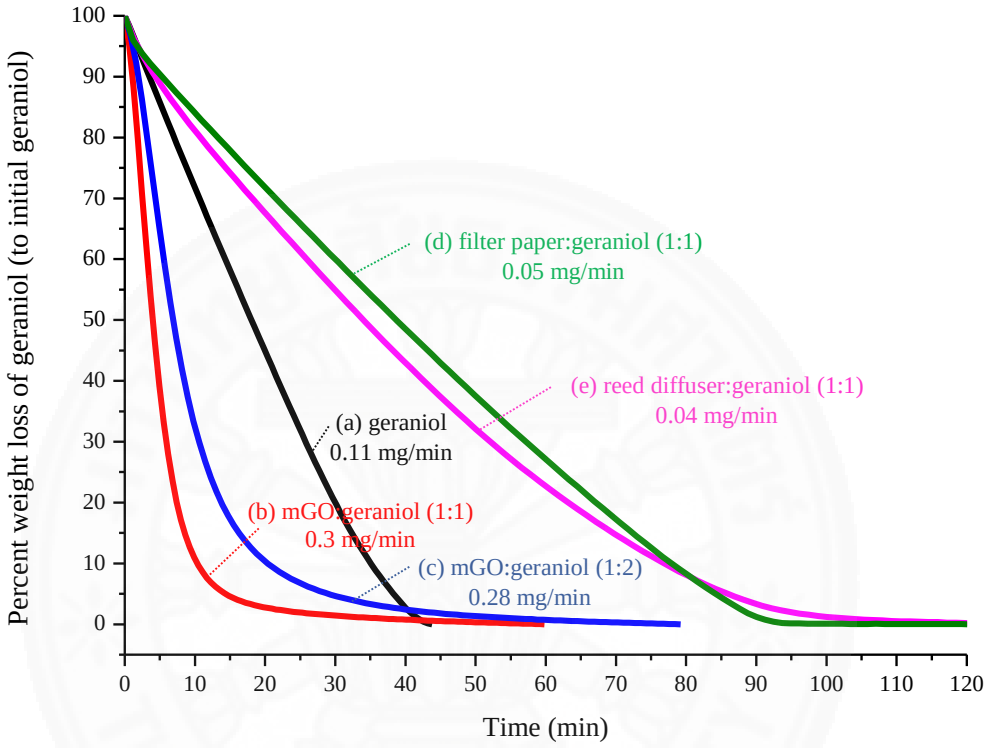

Figure 4.11 The average release rate of (a) geraniol, (b) geraniol-loaded mGO in the ratio of 1:1, and (c) 1:2, (d) geraniol-loaded filter paper in the ratio of 1:1, and (e) geraniol-loaded reed diffuser in the ratio of 1:1 at temperature **80°C**.

The release rate of geraniol on mGO shows a faster decay than the pure geraniol and geraniol on other sorbents. Release rate of pure geraniol from this graph is 0.11 mg/min. Geraniol-loaded mGO in the ratio of 1:1 and 1:2 have the release rate at 0.3 mg/min and 0.28 mg/min, respectively. And release rate of geraniol on filter paper and reed diffuser in the ratio of 1:1 are 0.05 mg/min and 0.04 mg/min, respectively.

It is interesting to note that mGO cannot decrease the average release rate but it accelerates the release rate of geraniol by about 2.7 times. In contrast, the curves of geraniol on filter paper and reed diffuser now show the slowest rate. Filter paper and reed diffuser can decrease the release rate of geraniol by about 2.4 times that means natural sorbents can slow down the release rate of geraniol. This is in the opposite trend to the earlier aroma compounds. This will be discussed in the FTIR and ^{1}H-NMR section. Geraniol probably does not prefer to be with mGO but it prefers to combine with natural sorbent such as filter paper and reed diffuser.

Ref. code: 25595722040614EIP

4.3 Loading efficiency and the actual percent loading of aroma compounds

The actual percent loading of aroma compounds can be obtained from TGA results by normalize the weight loss of composite to sample size, which be shown in the figure below.

The loading efficiency of aroma compounds is calculated as the ratio of the aroma compound that can actually be loaded to the amount of the aroma compound used in the preparation. Table 4.2 will shows the loading efficiency of all aroma compounds on the sorbents.

$$\text{Loading efficiency} = \frac{Actual\ amount\ of\ aroma\ compounds\ loaded\ (\%)}{Amount\ of\ aroma\ compounds\ used\ in\ preparation\ loading\ (\%)} \text{ x } 100\%$$

4.3.1 Menthol

From Figure 4.12, the menthol-loaded mGO has a slower release rate with a final weight of about 79%, equivalent to the menthol loading ratio of about 1:0.3. This is lower than the ratio used in the preparation (1:0.5 of the mGO weight: menthol weight), which means that not all menthol was loaded into the mGO during mixing probably because some of the menthol was loss due to evaporation during the heating up, or some menthol was attaching to the container's wall. Similarly, the menthol-loaded mGO at the ratio of 1:1 also has a final weight of about 55%, equivalent to the menthol loading ratio of about 1:0.9 lower than the ratio 1:1 used in the preparation.

The final weight of menthol-loaded reed diffuser is about 64%. This is equivalent to the actual loading of menthol in the reed diffuser of about 1:0.5. The filter paper also has a similar rate of weight decrease to that of the reed diffuser but with a lower final weight of about 54% equivalent to the menthol loading ratio of about 1:0.7 higher than the ratio used in the preparation (1:0.5 of filter weight: menthol weight), which is probably due to some moisture or volatile content in the filter paper used.

Ref. code: 25595722040614EIP

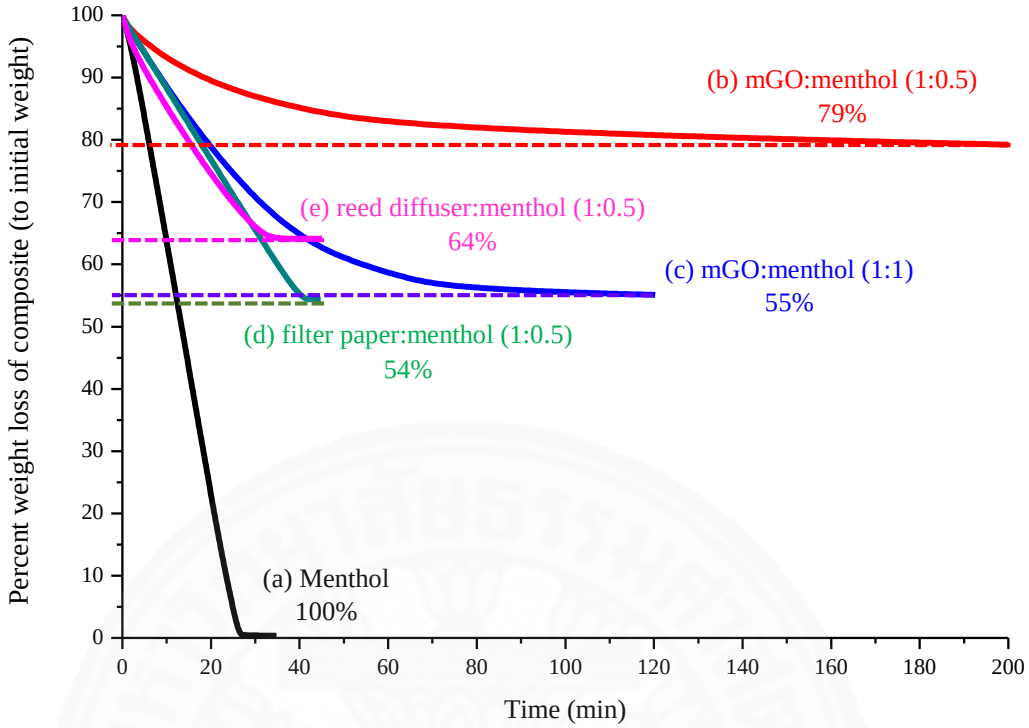

Figure 4.12 The percent amount of menthol loaded of (a) menthol, (b) menthol-loaded mGO in the ratio of 1:0.5, and (c) 1:1, (d) menthol-loaded filter paper in the ratio of 1:0.5, and (e) menthol-loaded reed diffuser in the ratio of 1:0.5. The temperature were at **80**°C.

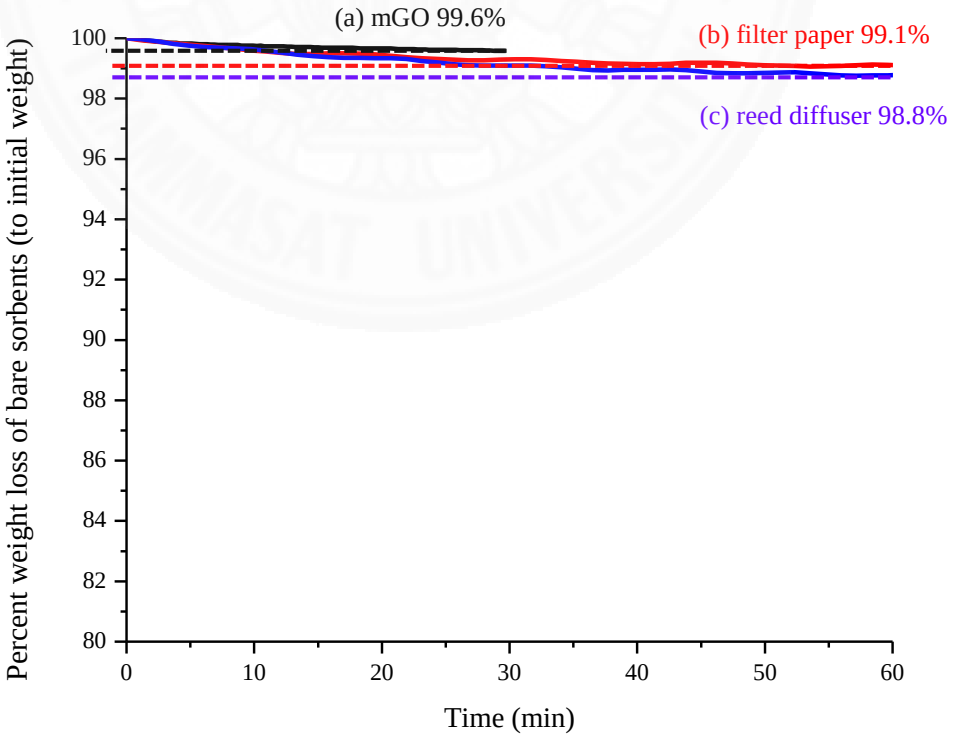

Figure 4.13 The percent amount of (a) mGO, (b) filter paper, and (c) reed diffuser. The temperature were at **80**°C.

Ref. code: 25595722040614EIP

For the bare sorbents in Figure 4.13, there is almost no weight change. The weight loss of the pure mGO is less than 0.5% during this time indicating that there is no significant weight change in pure mGO. While the weight losses of filter paper, and reed diffuser are less than 1.2%, slightly larger than that of the pure mGO but still very small and are insignificant compared to the weight of the menthol loaded.

4.3.2 Thymol

Actual percent loading of thymol-loaded mGO in the prepared ratio of 1:1 and 1:2 are shown in Figure 4.14. Their final weight of thymol-loaded mGO in the prepared ratio of 1:1 and 1:2 is about 67% and 47%, respectively. This is equivalent to the actual loading of thymol in mGO of about 1:0.7 for the prepared ratio 1:1, and 1:1.6 for the prepared ratio 1:2. This is lower than the ratio used in the preparation, which means that not all thymol was loaded into the mGO during mixing probably because some of the thymol was loss due to evaporation during the heating up, or some thymol was attached to the container's wall.

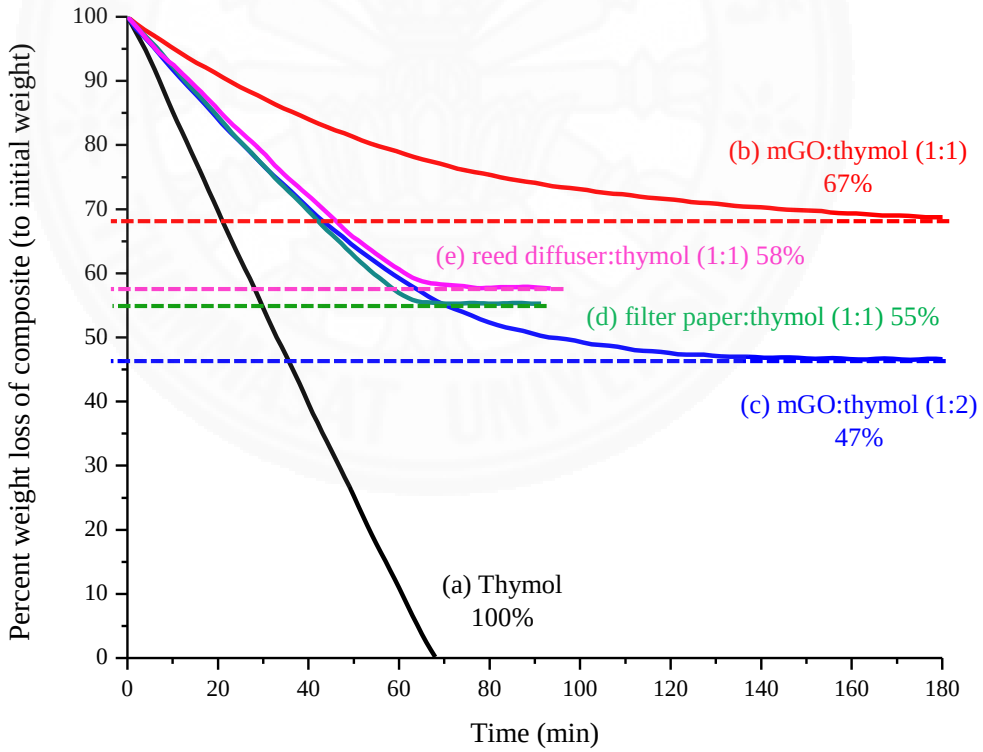

Figure 4.14 The percent amount of thymol loaded of (a) thymol, (b) thymol-loaded mGO in the ratio of 1:1, and (c) 1:2, (d) thymol-loaded filter paper in the ratio of 1:1, and (e) thymol-loaded reed diffuser in the ratio of 1:1. The temperature were at **80**℃.

Ref. code: 25595722040614EIP

Percent loading of filter paper-loaded thymol in the prepared ratio of 1:1 has a final weight of about 55%, equivalent to the thymol loading in the filter paper of about 1:0.9 similar to the ratio 1:1 used in the preparation. The reed diffuser also has a similar rate of weight decrease to that of the filter paper but with a higher final weight of about 58% equivalent to the thymol loading ratio of about 1:0.8 similar to the ratio used in the preparation (1:1 of reed diffuser weight: thymol weight). mGO can load thymol lower than that expected while reed diffuser and filter paper can load almost of thymol. Therefore, thymol prefers to combine with filter paper and reed diffuser more than mGO.

4.3.3 Citronellol

The percent weight loss of composites for citronellol are shown in Figure 4.15. The citronellol-loaded mGO has a slower release rate with a final weight of about 57%, equivalent to the citronellol loading ratio of about 1:0.9. This is similar to the ratio used in the preparation (1:1 of the mGO weight: citronellol weight). Similarly, the citronellol-loaded mGO at the ratio of 1:2 also has a final weight of about 37%, equivalent to the citronellol loading ratio of about 1:1.9 similar to the ratio 1:2 used in the preparation.

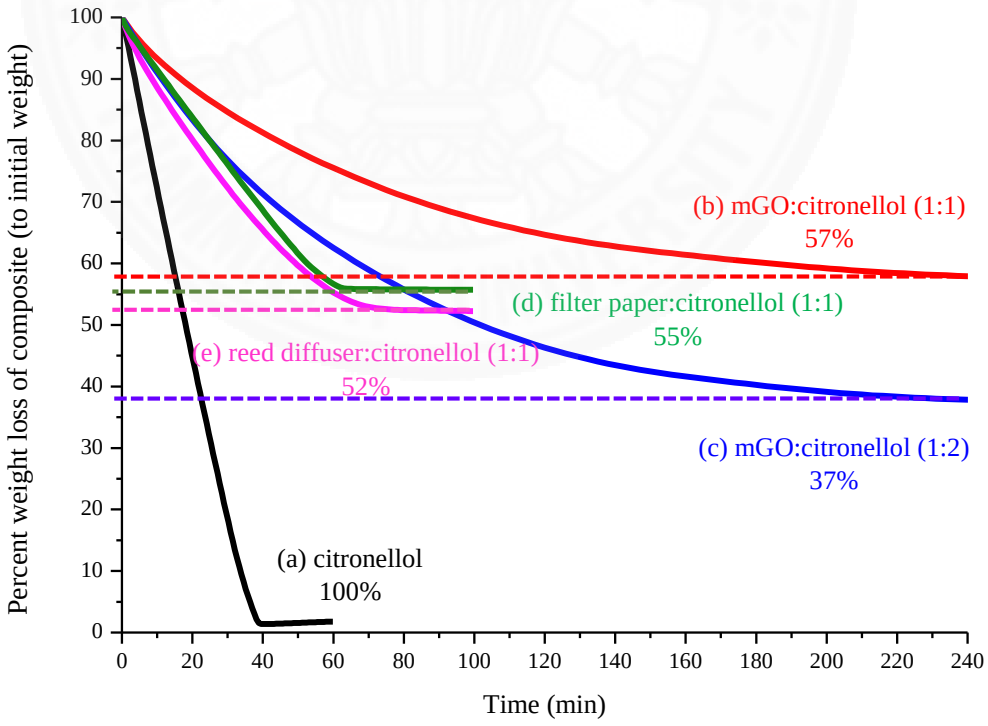

Figure 4.15 The percent amount of citronellol loaded of (a) citronellol, (b) citronellol-loaded mGO in the ratio of 1:1, and (c) 1:2, (d) citronellol-loaded filter paper in the ratio of 1:1, and (e) citronellol-loaded reed diffuser in the ratio of 1:1. The temperature were at **80**°C.

Ref. code: 25595722040614EIP

The weight loss of citronellol-loaded filter paper is slower than that of pure citronellol with the final weight of about 55%. This is equivalent to the actual loading of citronellol in the filter paper of about 1:0.9. The reed diffuser also has a similar rate of weight decrease to that of the filter paper but with a lower final weight of about 52% equivalent to the citronellol loading ratio of about 1:1 as the ratio used in the preparation (1:1 of reed diffuser weight: citronellol weight). These results show that mGO, filter paper, and reed diffuser can load citronellol as expected.

4.3.4 Geraniol

The percent weight loss of geraniol on sorbents are shown in Figure 4.16. The geraniol-loaded mGO has a final weight of about 71%, equivalent to the geraniol loading ratio of about 1:0.6. This is lower than the ratio used in the preparation (1:1 of the mGO weight: geraniol weight), which means that not all geraniol was loaded into the mGO during mixing probably because some of the geraniol was loss due to some geraniol was attaching to the container's wall. Similarly, the geraniol-loaded mGO at the ratio of 1:2 also has a final weight of about 52%, equivalent to the geraniol loading ratio of about 1:1.4 lower than the ratio 1:2 used in the preparation.

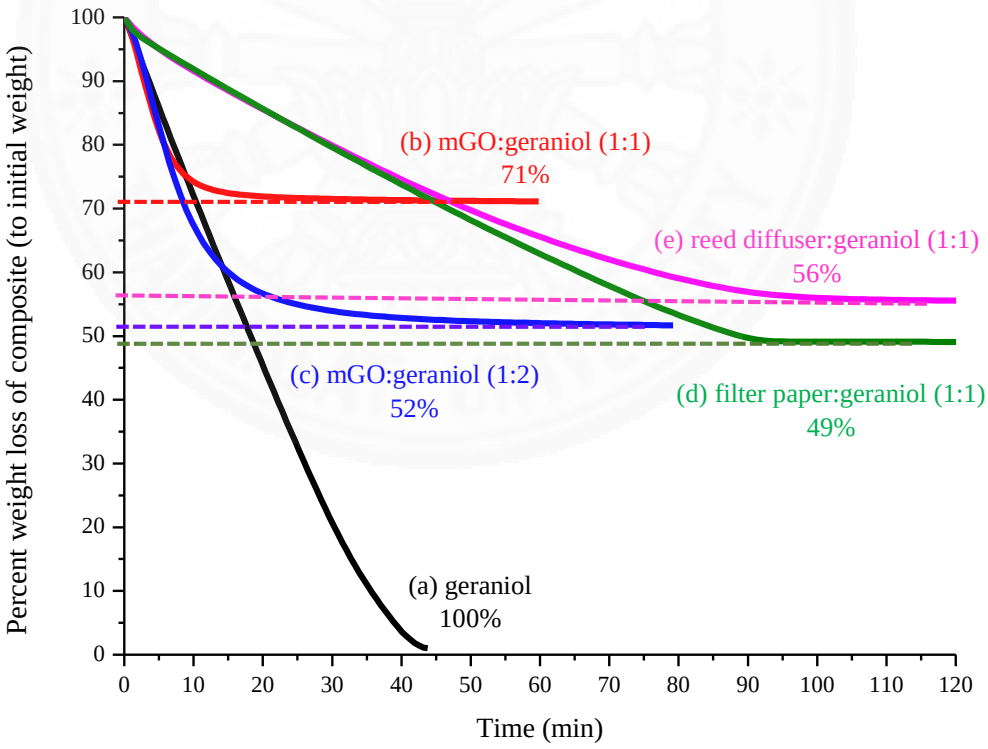

Figure 4.16 The percent amount of geraniol loaded of (a) geraniol, (b) geraniol-loaded mGO in the ratio of 1:1, and (c) 1:2, (d) geraniol-loaded filter paper in the ratio of 1:1, and (e) geraniol-loaded reed diffuser in the ratio of 1:1. The temperature were at **80**°C.

Ref. code: 25595722040614EIP

The filter paper also has a lower final weight of about 49% equivalent to the geraniol loading ratio of about 1:1 equal to the ratio used in the preparation (1:1 of filter weight: geraniol weight). Geraniol-loaded reed diffuser is slower than that of mGO with the final weight of about 56%. This is equivalent to the actual loading of geraniol in the reed diffuser of about 1:0.9. As a results, mGO cannot loaded all of the added geraniol while filter paper and reed diffuser can load geraniol as proposed.

Actual loading ratio of all aroma compounds on mGO, filter paper, and reed diffuser are summarized in Table 4.1.

Table 4.1 Actual loading ratio of all composites.

	Actual loading ratio						
	mGO			**Filter paper**		**Reed diffuser**	
Prepared ratio	**1:0.5**	**1:1**	**1:2**	**1:0.5**	**1:1**	**1:0.5**	**1:1**
Menthol	1:0.3	1:0.9	-	1:0.7	-	1:0.5	-
Thymol	-	1:0.6	1:1.6	-	1:0.9	-	1:0.8
Citronellol	-	1:0.8	1:1.9	-	1:0.9	-	1:0.9
Geraniol	-	1:0.6	1:1.4	-	1:1	-	1:0.9

Loading efficiency of all aroma compounds on the mGO, filter paper, and reed diffuser are shown in Table 4.2.

Table 4.2 Loading efficiency of aroma compounds on each sorbents.

	Loading efficiency (%)						
	mGO			**Filter paper**		**Reed diffuser**	
	1:0.5	1:1	1:2	1:0.5	1:1	1:0.5	1:1
Menthol	62	89	-	136	-	105	-
Thymol	-	65	80	-	88	-	83
Citronellol	-	84	93	-	87	-	94
Geraniol	-	55	68	-	101	-	87

Ref. code: 25595722040614EIP

In order to see clearer, Figure 4.17 was created. This figure shows the better loading efficiency of filter paper and reed diffuser than that of mGO. Which is probably due to some moisture or volatile content in the filter paper used being evaporated out and contributed to the aroma compounds weight loss in the TGA results.

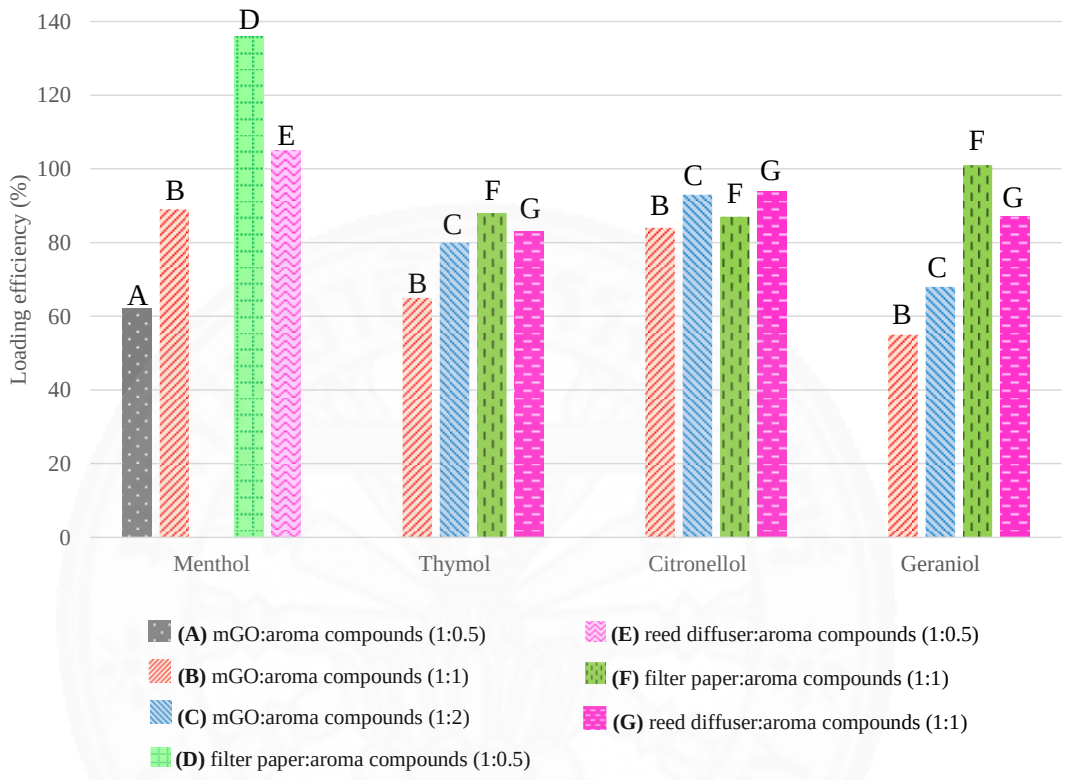

Figure 4.17 The loading efficiency of menthol, thymol, citronellol, and geraniol.

4.4 FTIR

Fourier Transform Infrared Spectroscopy (FTIR) was used to investigate the difference in chemical characteristics and interactions of sorbents after mix with aroma compounds.

4.4.1 Menthol

FTIR spectra in Figure 4.18 show band characteristics of functional groups as follow: 2949 cm^{-1} and 2866 cm^{-1} (methyl group, CH_3), 2915 cm^{-1} and 2845 cm^{-1} (methyl group, CH_2), 1043 cm^{-1} and 1024 cm^{-1} (C-O bonds), respectively [39]. These peaks can still be seen in all of menthol-loaded sorbent samples.

As expanded in Figure 4.19A and 4.19D, the spectrum of the subtraction curve between menthol-loaded mGO and mGO is shifted and broaden than other spectrum in the region of methyl group, in addition, the peak of the subtract mGO out spectrum at wavenumber 3241 cm^{-1} and 672 cm^{-1} in the region of -OH are disappears. Figure 4.19B

Ref. code: 25595722040614EIP

shows new peak at 1728 cm^{-1} of carbonyl group (C=O), these results are caused from oxidization of OH by mGO. From Figure 4.19C, the subtraction curve between menthol-loaded mGO and mGO at wavenumber 1043 cm^{-1}, and 1024 cm^{-1} in the region of C-O are shift to lower frequency and broaden, while filter paper and reed diffuser show no shift.

This indicates that menthol adsorbed onto the mGO interacts strongly with the mGO such that their peaks are shifted and also broaden, while those of traditional adsorbents such as the reed diffuser and the filter paper interact less strongly. Menthol has a planar aromatic benzene ring structure. The strong interaction between menthol and microwave graphene oxide may come from the good interaction between the menthol molecule and the planar structure of the reduced graphene oxide plane. The result that is also in the same trend as that of the menthol release rate observed in the TGA result.

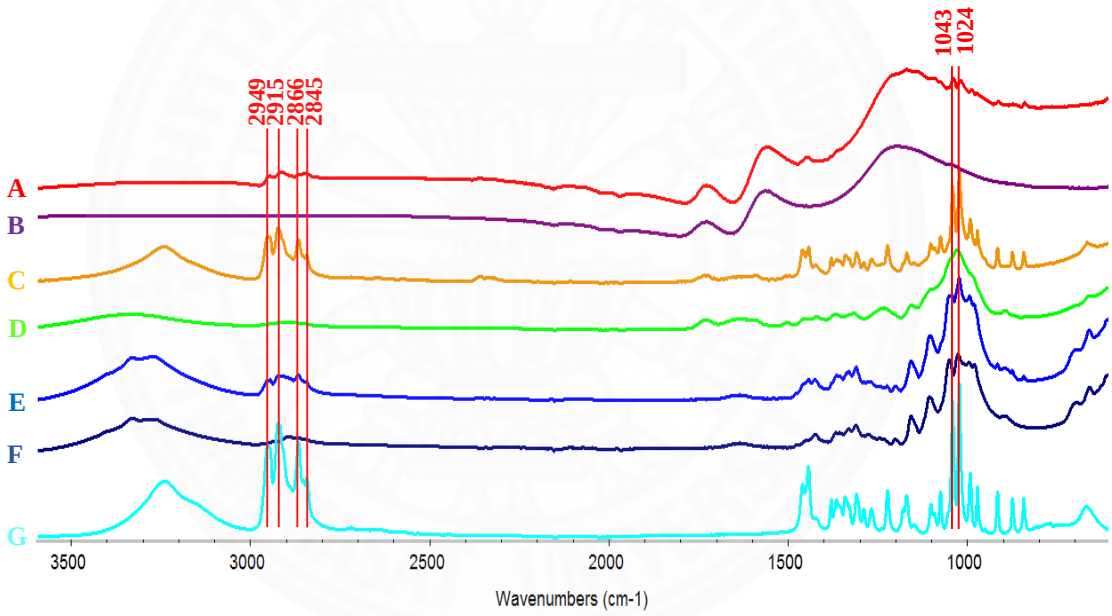

Figure 4.18 FTIR spectra of (A) menthol-loaded mGO, (B) mGO, (C) menthol-loaded reed diffuser, (D) reed diffuser, (E) menthol-loaded filter paper, (F) filter paper, and (G) menthol at wavenumber 3600-600 cm^{-1}.

Ref. code: 25595722040614EIP

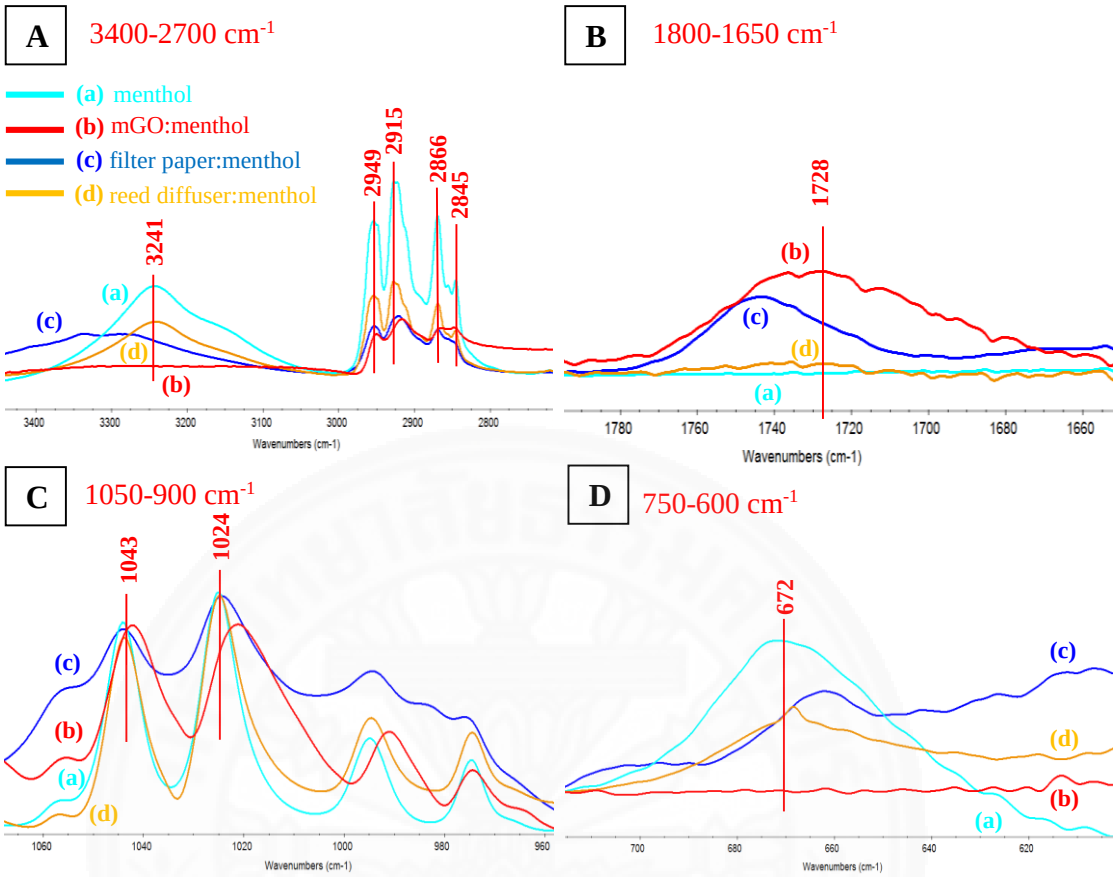

Figure 4.19 FTIR spectra of (a) menthol, and the subtraction spectra between the menthol-loaded sorbent and that of sorbent in order to show the FTIR spectra of the menthol on the sorbent of (b) menthol-loaded mGO, (c) menthol-loaded filter paper, and (d) menthol-loaded reed diffuser. A, B, C, D show the four different regions of the FTIR spectra at wavenumber 3400-2700 cm^{-1}, 1800-1650 cm^{-1}, 1050-900 cm^{-1}, and 750-600 cm^{-1}.

New peak of carbonyl group (C=O) in the subtraction curveof mGO shows that there may be an oxidation of menthol by mGO leading to the new C=O bond formed and the loss of the alcohol (–OH) group. There are some reviews about the reaction of menthol that they can react in many ways like a normal secondary alcohol, it can be oxidized to menthone by an oxidizing agent, and under some conditions oxidation can even break open the ring [40]. One of the oxidation products of menthol may be menthone. Menthone is also used in perfumes and artificial flavors and has smell quite similar to that of menthol [41, 42].

Ref. code: 25595722040614EIP

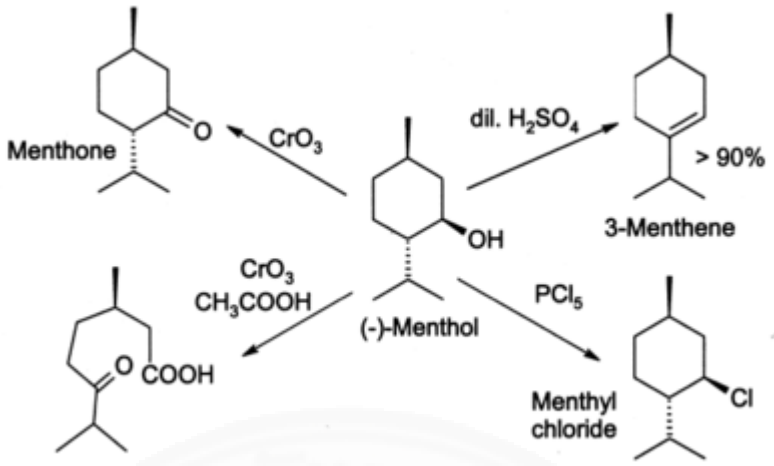

Figure 4.20 Reaction of menthol [40].

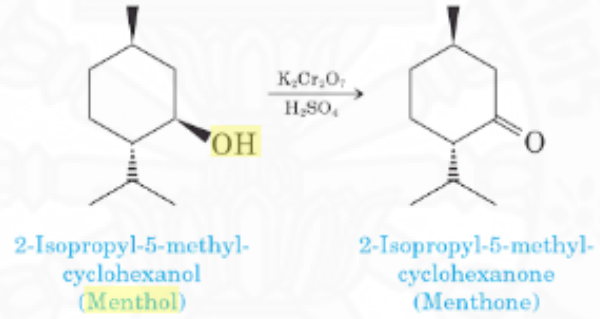

Figure 4.21 Oxidation of menthol to menthone [41, 42].

4.4.2 Thymol

FTIR spectra of thymol, and thymol on sorbents are shown in Figure 4.22. Thymol has several strong and sharp peaks which can be assigned to characteristic functional groups of 2960 cm^{-1}(methyl group, CH_3), 2928 cm^{-1}, 2868 cm^{-1}, 1463 cm^{-1}, and 740 cm^{-1} (methyl group, CH_2), 1622 cm^{-1} (C=C), 1418 cm^{-1} (C-O-H), 1241 cm^{-1} and 1160 cm^{-1} (C-O), 938 cm^{-1} (OH bend), and 808 cm^{-1} (C=C), respectively. These peaks can still be seen in the thymol-loaded sorbent samples.

In order to see the difference clearer, subtraction spectra of the thymol-loaded samples in the region of strong thymol peaks around 1500-1100 cm^{-1} are shown in Figure 4.23. The spectrum of the subtraction curve between thymol-loaded mGO and mGO is minimal shift. There are minimal change in intensity and band patterns of C-O stretch at wavenumber 1241 cm^{-1} for subtraction curves of all sorbent samples. FTIR results demonstrate minimal interaction between thymol and all sorbents including mGO, filter paper, and reed diffuser.

Ref. code: 25595722040614EIP

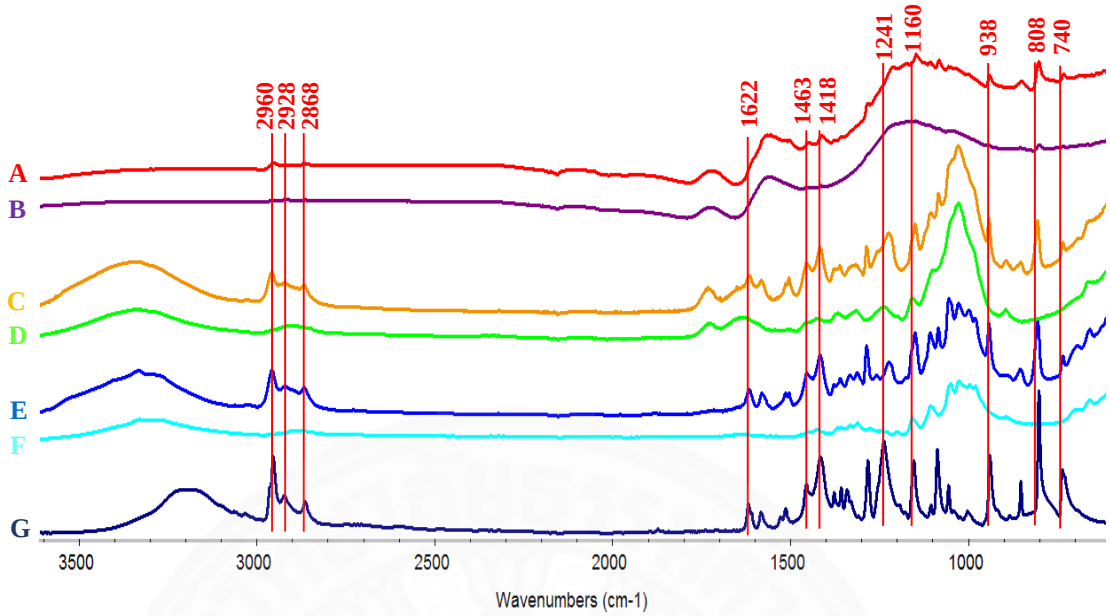

Figure 4.22 FTIR spectra of (A) thymol-loaded mGO, (B) mGO, (C) thymol-loaded reed diffuser, (D) reed diffuser, (E) thymol-loaded filter paper, (F) filter paper, and (G) thymol at wavenumber 3600-600 cm^{-1}.

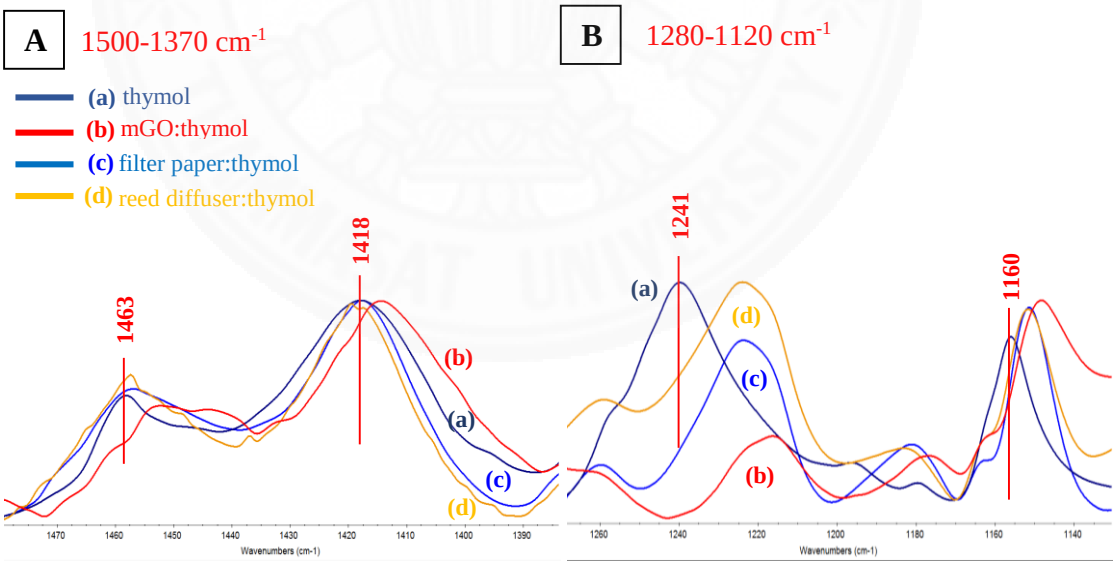

Figure 4.23 FTIR spectra of (a) thymol, and the subtraction spectra between the thymol-loaded sorbent and that of sorbent in order to show the FTIR spectra of the thymol on the sorbent of (b) thymol-loaded mGO, (c) thymol-loaded filter paper, and (d) thymol-loaded reed diffuser. A, B show the two different regions of the FTIR spectra at wavenumber 1500-1370 cm^{-1}, and 1280-1120 cm^{-1}.

Ref. code: 25595722040614EIP

4.4.3 Citronellol

The spectra as expended in Figure 4.24 show band characteristics of functional groups as follow: 2962 cm^{-1}, 2870 cm^{-1}, and 1378 cm^{-1} (methyl group, CH_3), 2914 cm^{-1}, 2855 cm^{-1}, and 1450 cm^{-1} (methyl group, CH_2), and 1056 cm^{-1} (C-O bond), respectively. These peaks can still be seen in the citronellol-loaded sorbent samples. Subtraction spectra by subtract substrate out in Figure 4.25 show that the subtraction spectra of citronellol-loaded mGO and citronellol-loaded reed diffuser are minimal shift at wavenumber 3000-2800 cm^{-1} and 1080-960 cm^{-1} in the region of CH and C-O bonds. FTIR results indicate that citronellol on sorbents has a minimal change which is not effects.

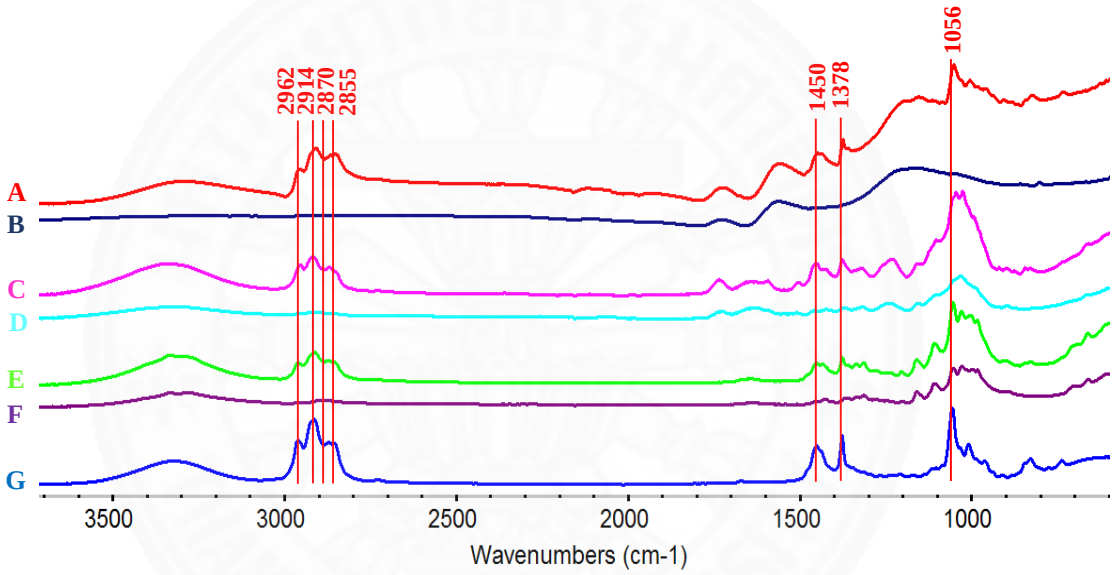

Figure 4.24 FTIR spectra of (A) citronellol-loaded mGO, (B) mGO, (C) citronellol-loaded reed diffuser, (D) reed diffuser, (E) citronellol-loaded filter, (F) filter paper, and (G) citronellol at wavenumber 3600-600 cm^{-1}.

Ref. code: 25595722040614EIP

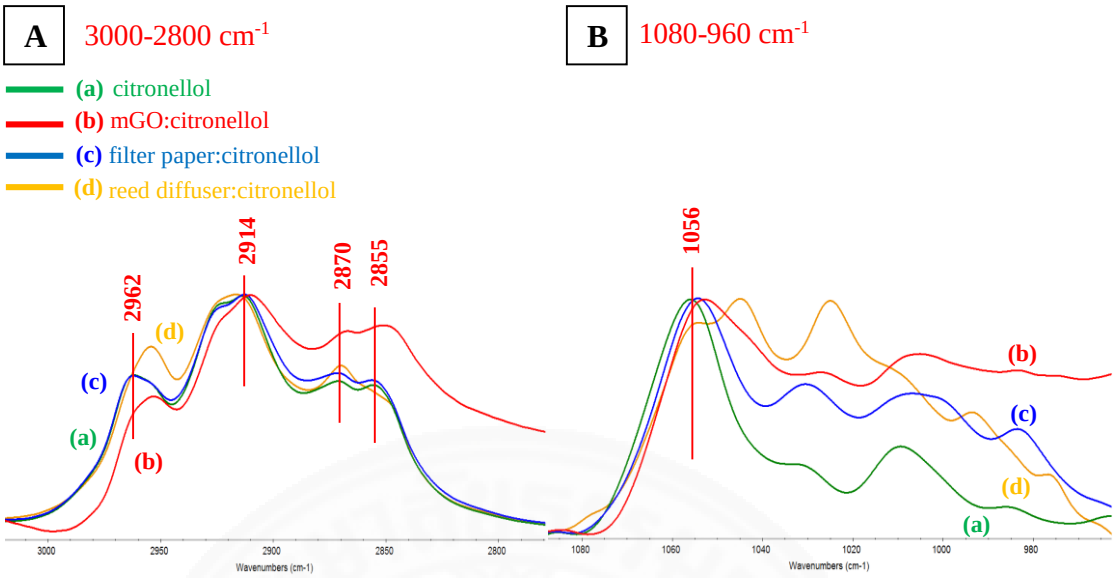

Figure 4.25 FTIR spectra of (a) citronellol, and the subtraction spectra between the citronellol-loaded sorbent and that of sorbent in order to show the FTIR spectra of the citronellol on the sorbent of (b) citronellol-loaded mGO, (c) citronellol-loaded filter paper, and (d) citronellol-loaded reed diffuser. A, B show the two different regions of the FTIR spectra at wavenumber 3000-2800 cm^{-1}, and 1080-960 cm^{-1}.

4.4.4 Geraniol

FTIR spectra of geraniol, sorbents, and geraniol on sorbents are shown in Figure 4.26. Geraniol has several strong and sharp peaks which can be assigned to characteristic functional groups of 2965 cm^{-1}, 2880 cm^{-1}, and 1376 cm^{-1} (methyl group, CH_3), 2915 cm^{-1}, 2855 cm^{-1}, and 1440 cm^{-1} (methyl group, CH_2), 1668 cm^{-1} (-C=C-), 1096 cm^{-1} (C-O-H), and 995 cm^{-1} (-C=CH), respectively. These peaks can still be seen in the geraniol-loaded sorbent samples.

In order to see the difference clearer, the subtraction spectra by subtracting the FTIR spectrum of the substrate out are shown in Figure 4.27. The spectrum of the subtraction curve between geraniol-loaded mGO and mGO shows significantly lower intensity than other sorbents in the region of -C=CH at the wavenumber 995cm^{-1}. In addition, there is a new peak in the region of CH at wavenumber 920 cm^{-1}.

Ref. code: 25595722040614EIP

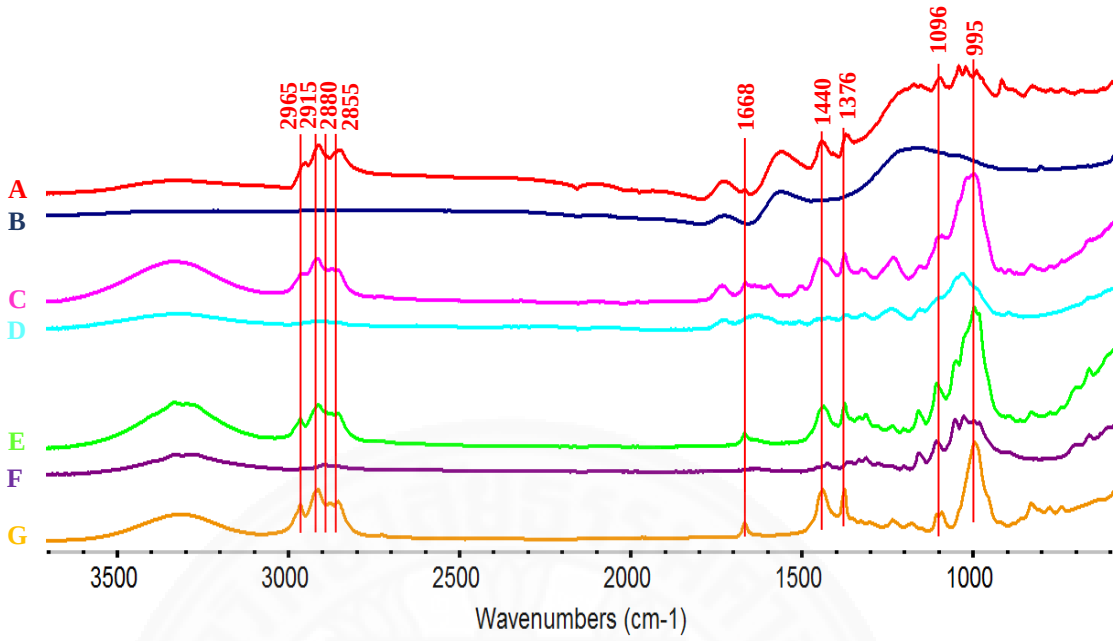

Figure 4.26 FTIR spectra of (A) geraniol-loaded mGO, (B) mGO, (C) geraniol-loaded reed diffuser, (D) reed diffuser, (E) geraniol-loaded filter paper, (F) filter paper, and (G) geraniol at wavenumber 3600-600 cm^{-1}.

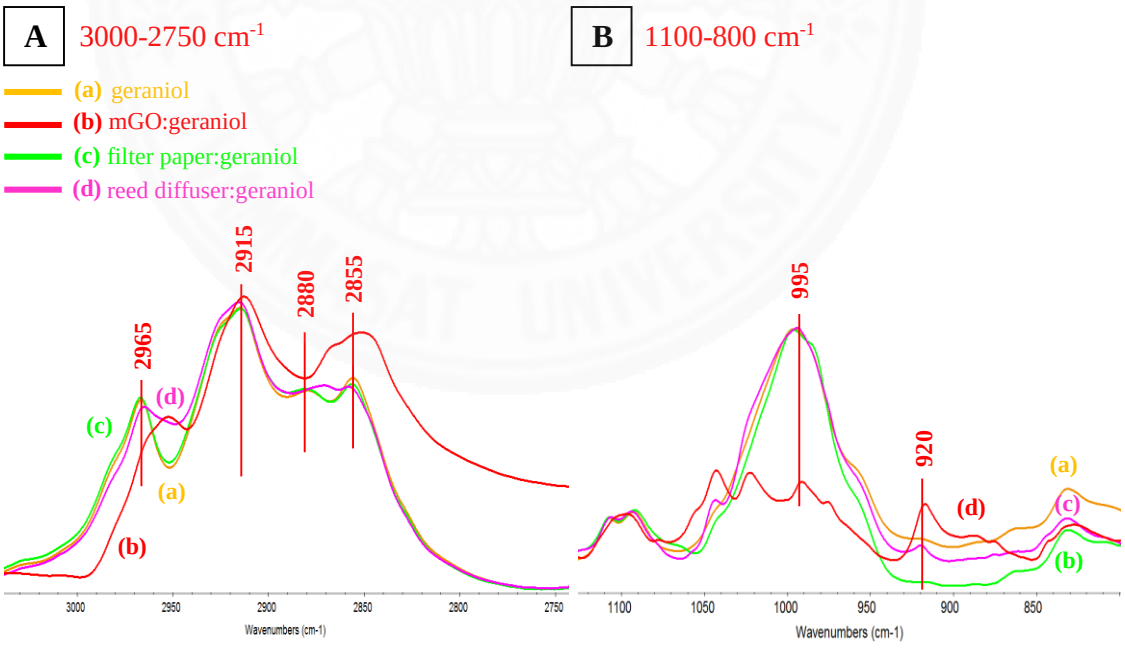

Figure 4.27 FTIR spectra of (a) geraniol, and the subtraction spectra between the geraniol-loaded sorbent and that of sorbent in order to reveal the FTIR spectra of the geraniol on the sorbent of (b) geraniol-loaded mGO, (c) geraniol-loaded filter paper, and (d) geraniol-loaded reed diffuser. A, B show the two different regions of the FTIR spectra at wavenumber 3000-2750 cm^{-1}, and 1100-800 cm^{-1}.

Ref. code: 25595722040614EIP

These results indicate that mGO may react with geraniol causing changes in the geraniol structure. Moreover, the physical smell have a noticeable change from the rose odor to the lemon odor.

Products of oxidation of geraniol or nerol is shown in Figure 4.28. Nerol is the trans-isomer of the geraniol (geraniol is cis). Geranial (citral A) and Neral (citral B) are primary oxidation products of geraniol/nerol. They are an important intermediate for production of perfumed, and pharmaceuticals [43]. Molecular formular of citral is $C_{10}H_{16}O$, it provides a lemon-like odor [44].

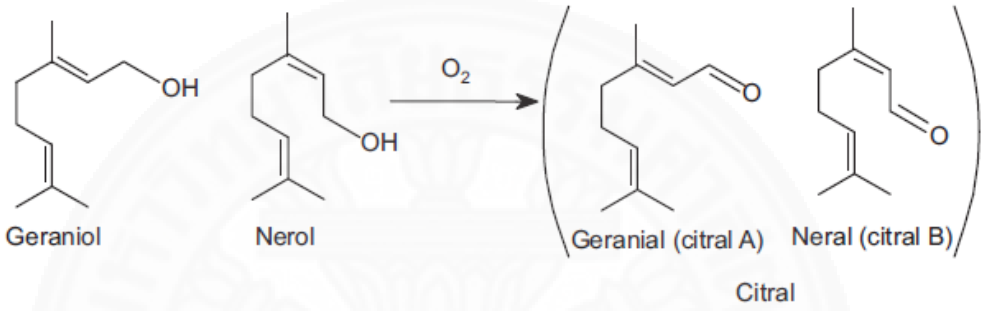

Figure 4.28 Products of oxidation of geraniol [43].

4.5 ^{1}H-NMR

Proton nuclear magnetic resonance (^{1}H-NMR) of the materials are shown in Figure 4.29-4.34. Figure 4.29 shows proton NMR of mGO, it has a signal of benzene ring around 5-7 ppm, OH at 7.223 ppm, and CH_3 at 1.599 ppm. ^{1}H-NMR of menthol in Figure 4.30 shows the signal of CH at 3.393 ppm, 2.147 ppm, 1.955 ppm, and 1.471 ppm, CH_2 at 1.602 ppm, 1.090 ppm, and 1.086 ppm, and CH_3 at 0.913 ppm, 0.898 ppm, and 0.795 ppm. Menthol-loaded mGO in the ratio of 1:1 shows higher peak of CH at 1.471 ppm when normalized by CH at 3.393 ppm (A position), this peak is related to position F in the structure of menthol. This means proton signal at position F increase probably because mGO reacts with the hydroxyl group (-OH) of menthol. These results also correlate with FTIR results that there are oxidation of menthol.

Ref. code: 25595722040614EIP

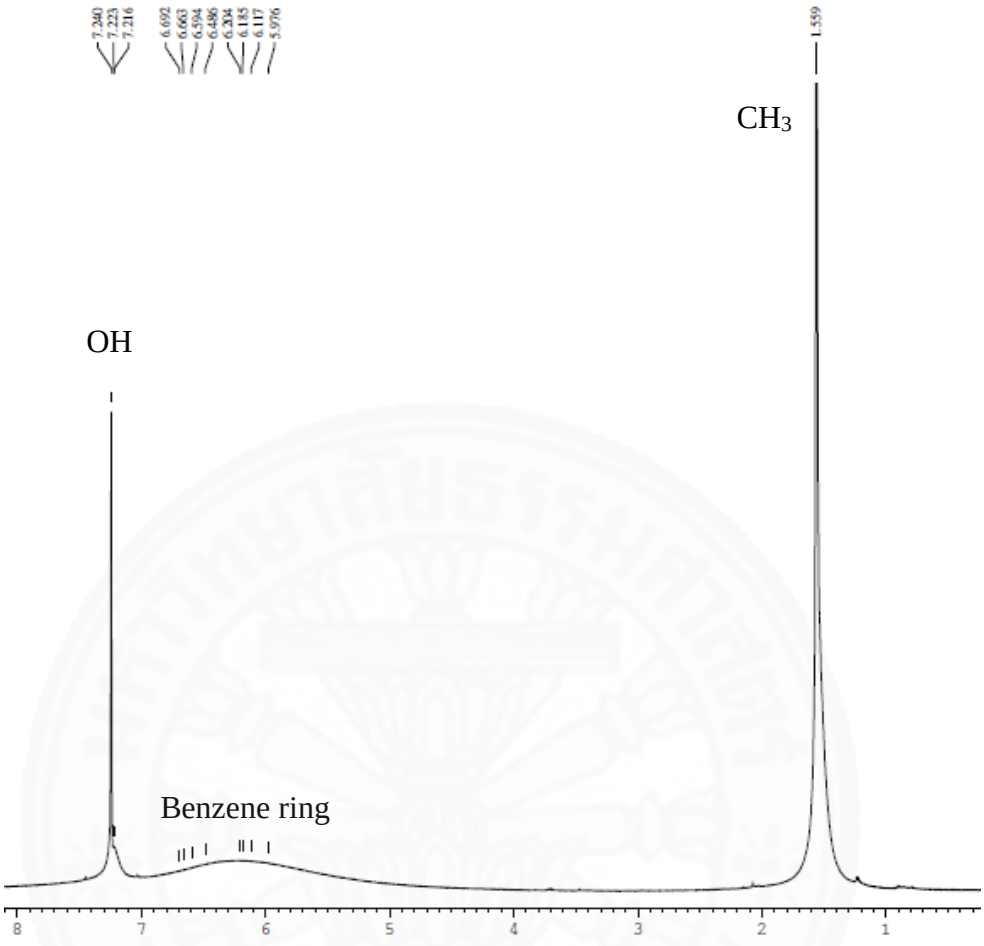

Figure 4.29 ^{1}H-NMR of mGO.

Ref. code: 25595722040614EIP

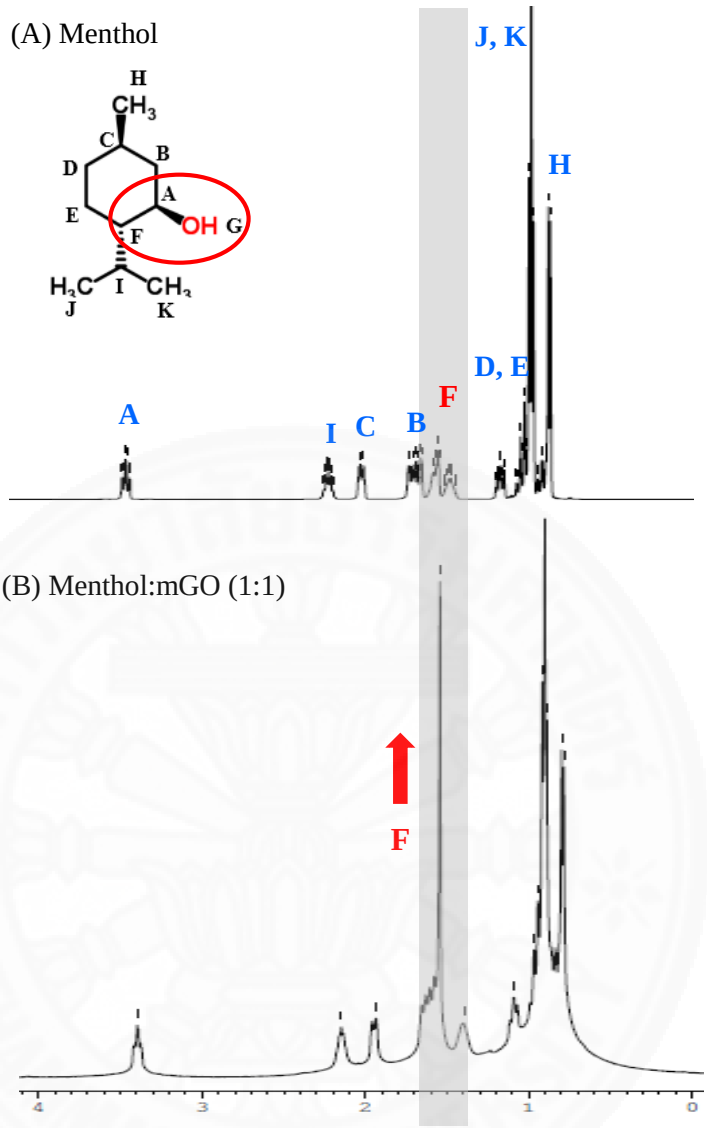

Figure 4.30 ^{1}H-NMR of (A) menthol, and (B) menthol-loaded mGO.

Proton NMR results of thymol and thymol-loaded mGO are shown in Figure 4.31, there is no significant difference between the two graphs. This means that there is no chemical change in the structure of the thymol on mGO, they have only physical absorption. The structure of thymol is benzene ring which is same as mGO, and they are still benzene ring structure after loading. This is the reason why the release rate of thymol-loaded mGO is slightly changed.

Ref. code: 25595722040614EIP

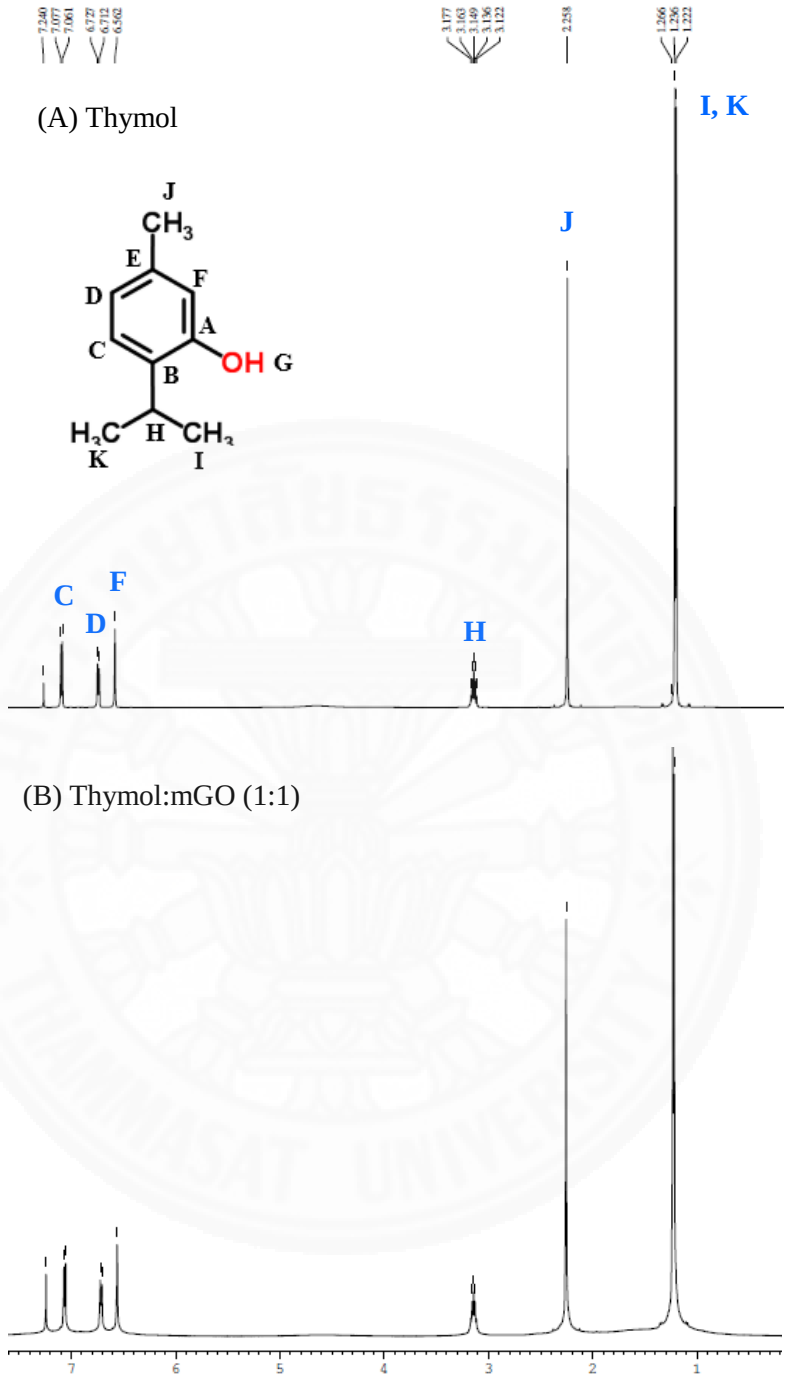

Figure 4.31 ^{1}H-NMR of thymol, and thymol-loaded mGO.

The ^{1}H-NMR of citronellol and citronellol-loaded mGO in the ratio of 1:1 are shown in Figure 4.32. There are a minimal increase of proton signals at 1.433 ppm, 1.372 ppm and 1.176 ppm (F position) when normalized by CH at 7.077 ppm (C position). mGO does not seem to cause much changes in the chemical structure of the citronellol.

Ref. code: 25595722040614EIP

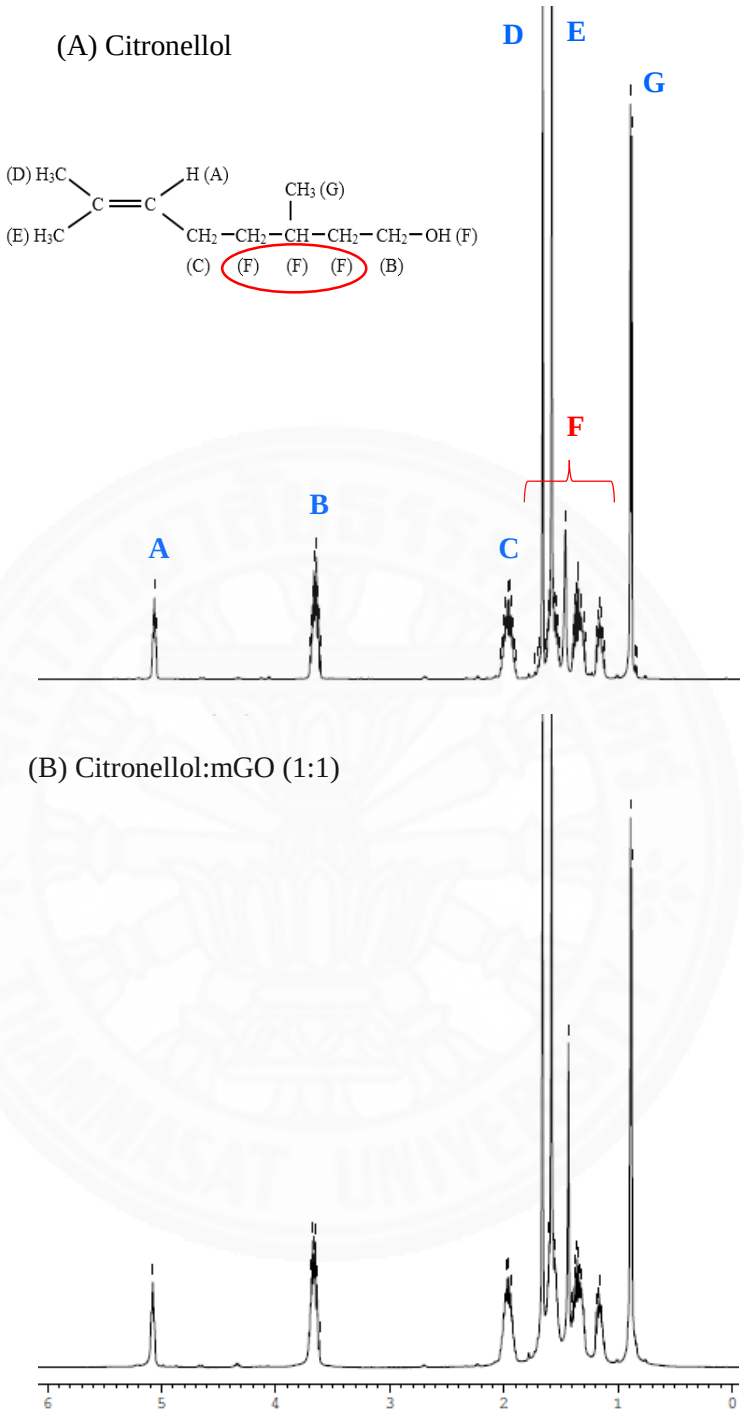

Figure 4.32 ^{1}H-NMR of (A) citronellol, and (B) citronellol-loaded mGO.

The proton NMR of geraniol and geraniol-loaded mGO in the ratio of 1:1 are shown in Figure 4.33. Geraniol has a prominent peak of CH at 5.392 ppm (A), 5.069 ppm (B), CH_2 at 4.135 ppm (C), 2.101-1.990 ppm (D), and CH_3 at 1.655 ppm (E), and 1.580 ppm (F). When normalized by CH at 5.069 ppm (B), the intensity of CH at 5.397 ppm (A) and CH_2 at 4.135 ppm (C) in the geraniol-loaded mGO is reduced. This results

Ref. code: 25595722040614EIP

may be caused from the oxidation of geraniol. The chemical structure of geraniol may be broken and changed by mGO which may also causes the fast release rate of geraniol observed in the TGA results.

The ^{1}H-NMR signals of geraniol-loaded reed diffuser and reed diffuser are shown in Figure 4.34. There is no significant change in the structure of geraniol after loading onto the reed diffuser. Geraniol is not changed by the reed diffuser, and this is in the same trend as the release rate which did not change significantly.

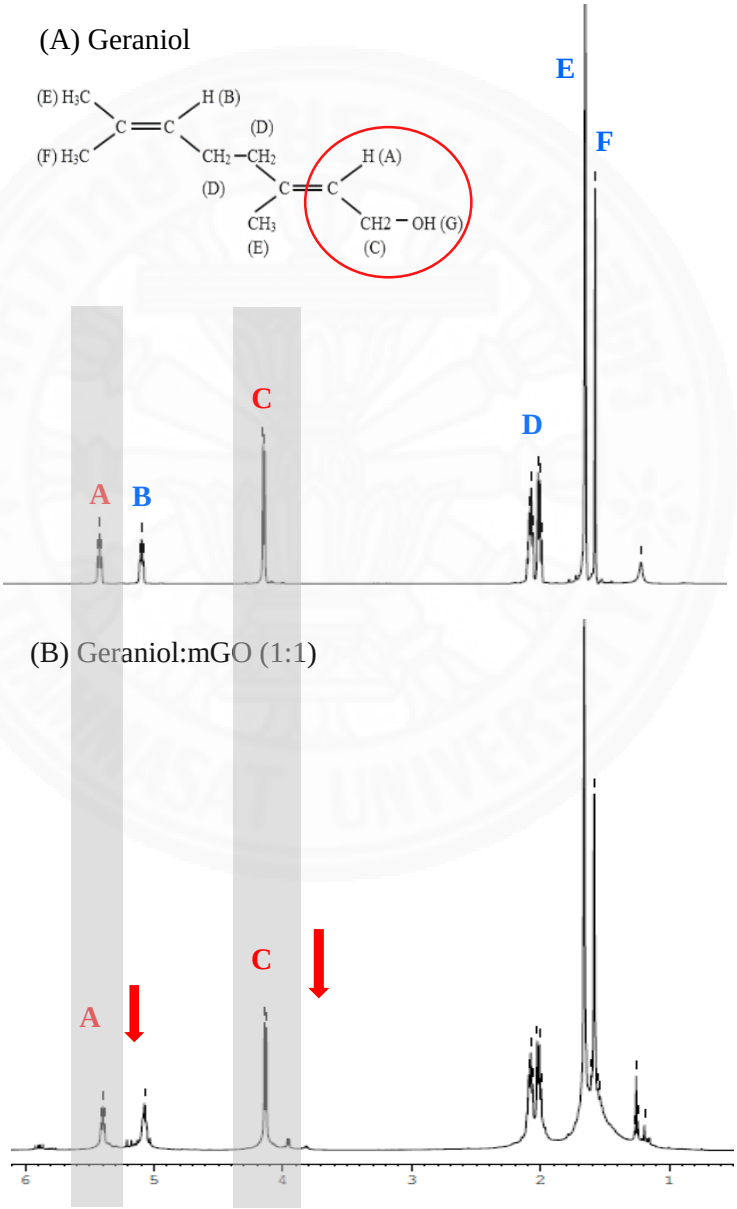

Figure 4.33 ^{1}H-NMR of (A) geraniol, and (B) geraniol-loaded mGO.

Ref. code: 25595722040614EIP

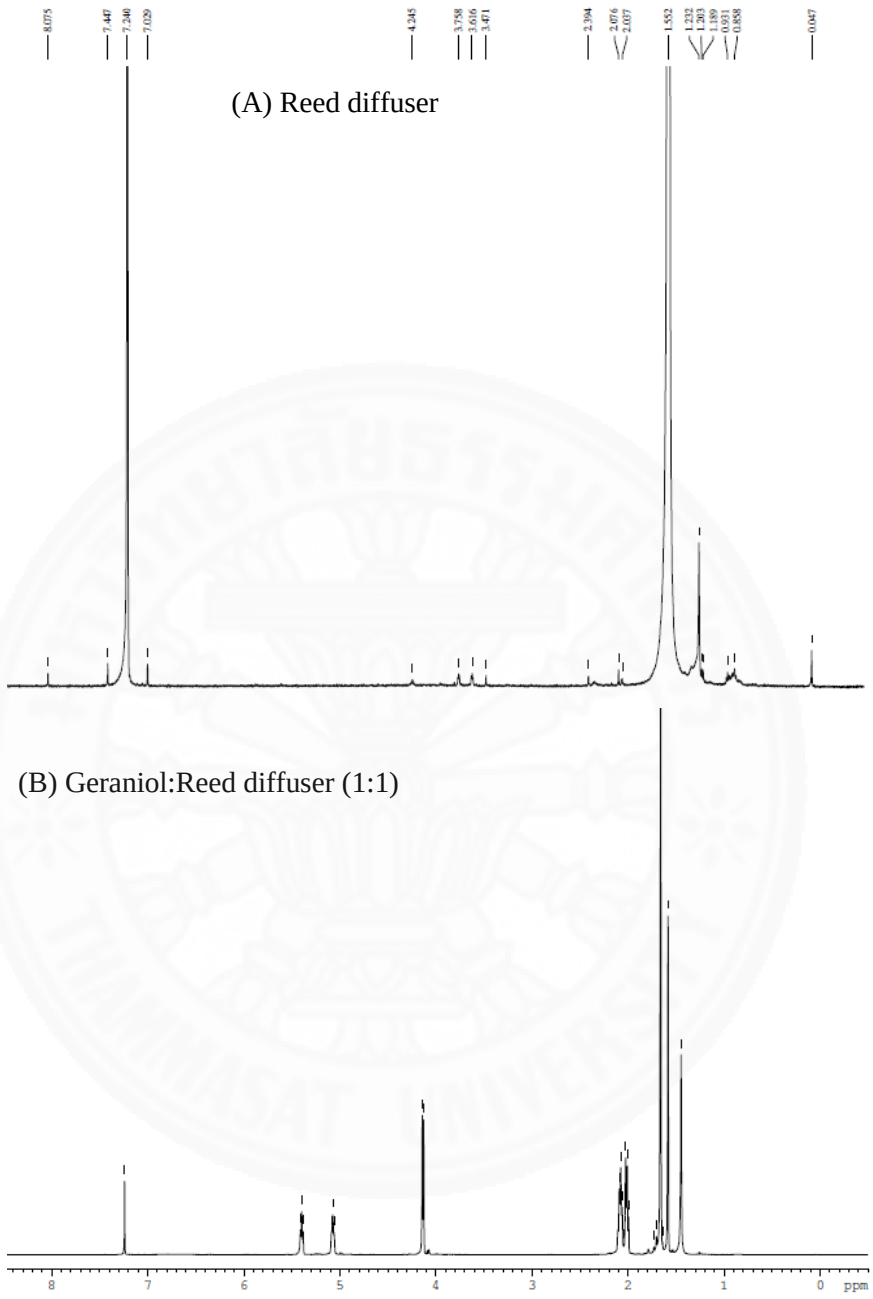

Figure 4.34 ^{1}H-NMR of (A) reed diffuser, and (B) geraniol-loaded reed diffuser.

Ref. code: 25595722040614EIP

4.6 X-ray Diffraction (XRD)

4.6.1 Menthol

Figure 4.35 shows the intensity of menthol, mGO, menthol-loaded mGO in the ratio of 1:1 and 1:2, filter paper, and menthol-loaded filter paper in the ratio of 1:1. Menthol-loaded mGO in the ratio of 1:2 has the crystalline peaks of menthol at the 2-theta between 7 to 25 degrees same as 1:1 menthol-loaded filter paper. In contrast, menthol-loaded mGO in the ratio of 1:1 has no crystalline peak of menthol and it similar to the intensity of mGO. XRD results indicated that in the ratio of 1:1, mGO can combine with menthol completely, and mGO cannot load all of menthol more than 1 times that of menthol. While filter paper can load the menthol lower than 1 times.

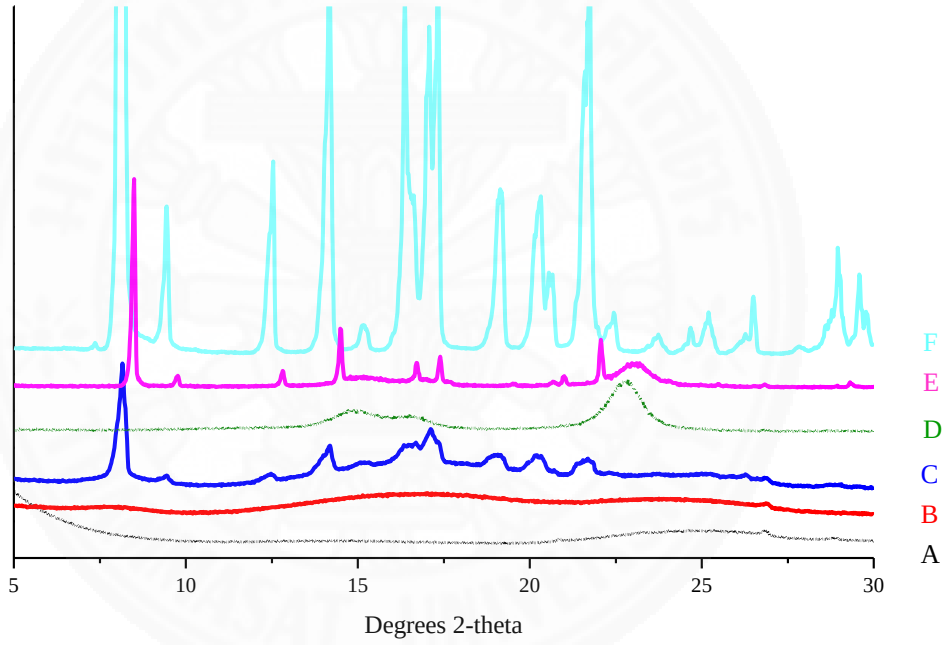

Figure 4.35 XRD patterns of (A) mGO, (B) menthol-loaded mGO in the ratio of 1:1, (C) menthol-loaded mGO in the ratio of 1:2, (D) filter paper, (E) menthol-loaded filter paper in the ratio of 1:1, and (F) menthol at 5-30 degrees 2-theta.

Crystalline index (CI) can be calculated from XRD results using fityk program. This program provides crystal area, amorphous area, and total area, which CI can be calculated from crystal area divided by total area and multiplied by 100. The calculated data shows in table 4.3, CI of menthol-loaded mGO in the ratio of 1:1 is not detectable, but in the ratio of 1:2 is 32. In contrast, menthol-loaded filter paper is 100. This results support the XRD graph.

Ref. code: 25595722040614EIP

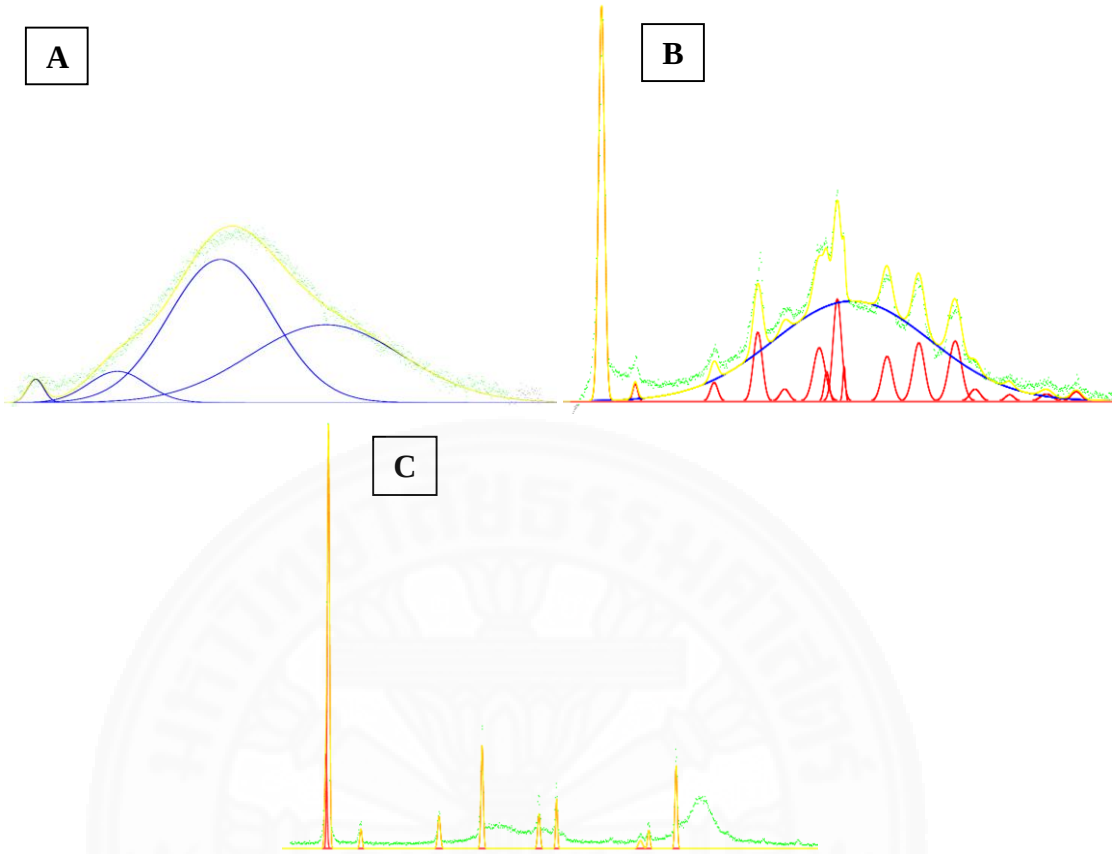

Figure 4.36 Crystalline index (CI) of (A) menthol-loaded mGO in the ratio of 1:1, and (B) 1:2, and (C) menthol-loaded filter paper in the ratio of 1:1 at 7-25 degrees 2-theta from fityk program.

Table 4.3 Crystalline index (CI) of menthol-loaded mGO in the ratio of 1:1, and 1:2, and menthol-loaded filter paper in the ratio of 1:1.

	mGO:menthol (1:1)	**mGO:menthol (1:2)**	**Filter paper:menthol (1:1)**
Crystal area	0	27692	1271
Amorphous area	56021	60060	0
Total area	56021	87752	1271
CI	**0**	**32**	**100**

Ref. code: 25595722040614EIP

4.6.2 Thymol

Figure 4.37 shows the intensity of thymol, mGO, thymol-loaded mGO in the ratio of 1:1 and 1:2, filter paper, and thymol-loaded filter paper. All of composites have no crystalline peak of thymol. XRD results indicated that thymol does not form crystal of thymol after loaded onto sorbents.

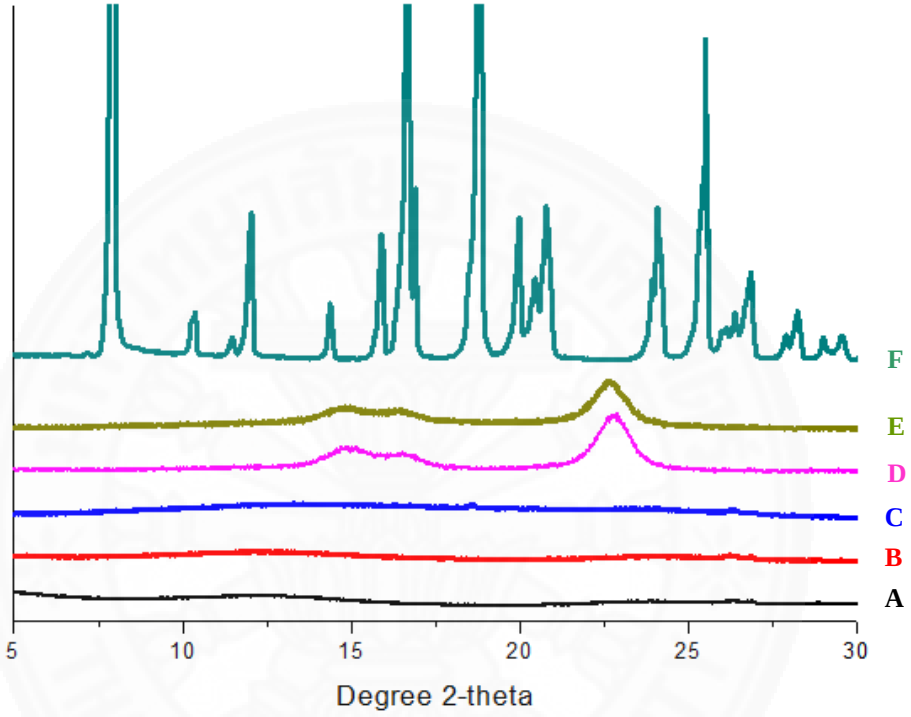

Figure 4.37 XRD patterns of (A) mGO, (B) thymol-loaded mGO in the ratio of 1:1, and (C) 1:2, (D) filter paper, (E) thymol-loaded filter paper in the ratio of 1:1, and (F) thymol.

For geraniol and citronellol, they are in liquid form and therefore do not have XRD results.

4.7 Differential Scanning Calorimetry (DSC)

DSC curves of menthol are shown in Figure 4.38. Menthol has a melting peak at 44.26 °C. Composites of filter paper and reed diffuser present melting peak of menthol near the menthol melting point. While menthol-loaded mGO has no melting peak, that means mGO can absorb menthol completely.

Ref. code: 25595722040614EIP

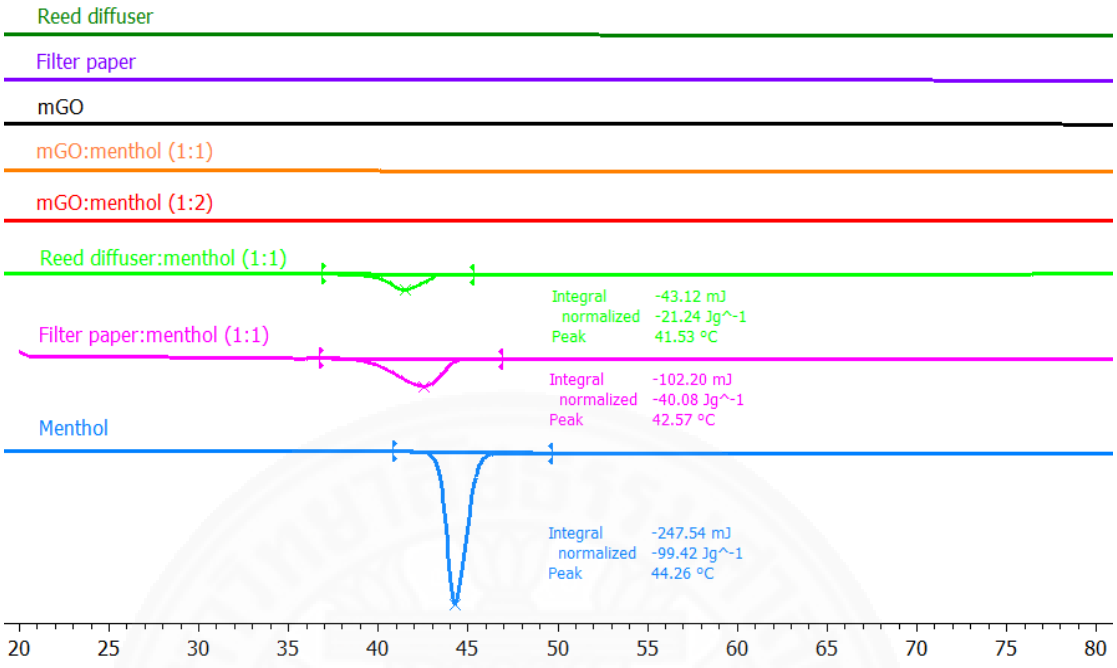

Figure 4.38 DSC curves of menthol.

For thymol in Figure 4.39, there is melting peak of thymol at 51.20 °C, but there are no same peak of the thymol on the thymol-loaded mGO and thymol-loaded reed diffuser.

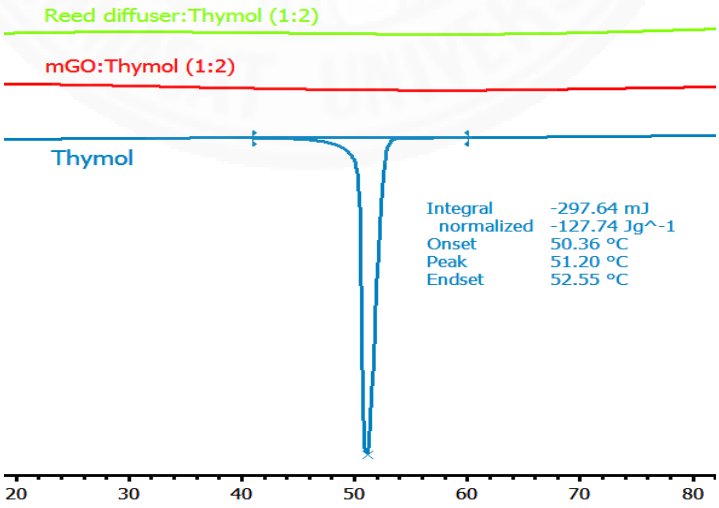

Figure 4.39 DSC curves of thymol.

Ref. code: 25595722040614EIP

4.8 Specific surface area

Brunauer-Emmett-Teller (BET) theory is used to reveal specific surface area of sorbents. BET-plot of mGO are shown in Figure 4.40, specific surface area of mGO is 543 m^2/g at a correlation coefficient of 0.9982. This result shows that mGO has quite high specific surface area. Conversary, filter paper has a very low specific surface area which is -2 m^2/g at a correlation coefficient of -0.9996. This error of filter paper may cause from very low specific surface area. Specific surface area of reed diffuser is 0.29 m^2/g at a correlation coefficient of 0.9981.

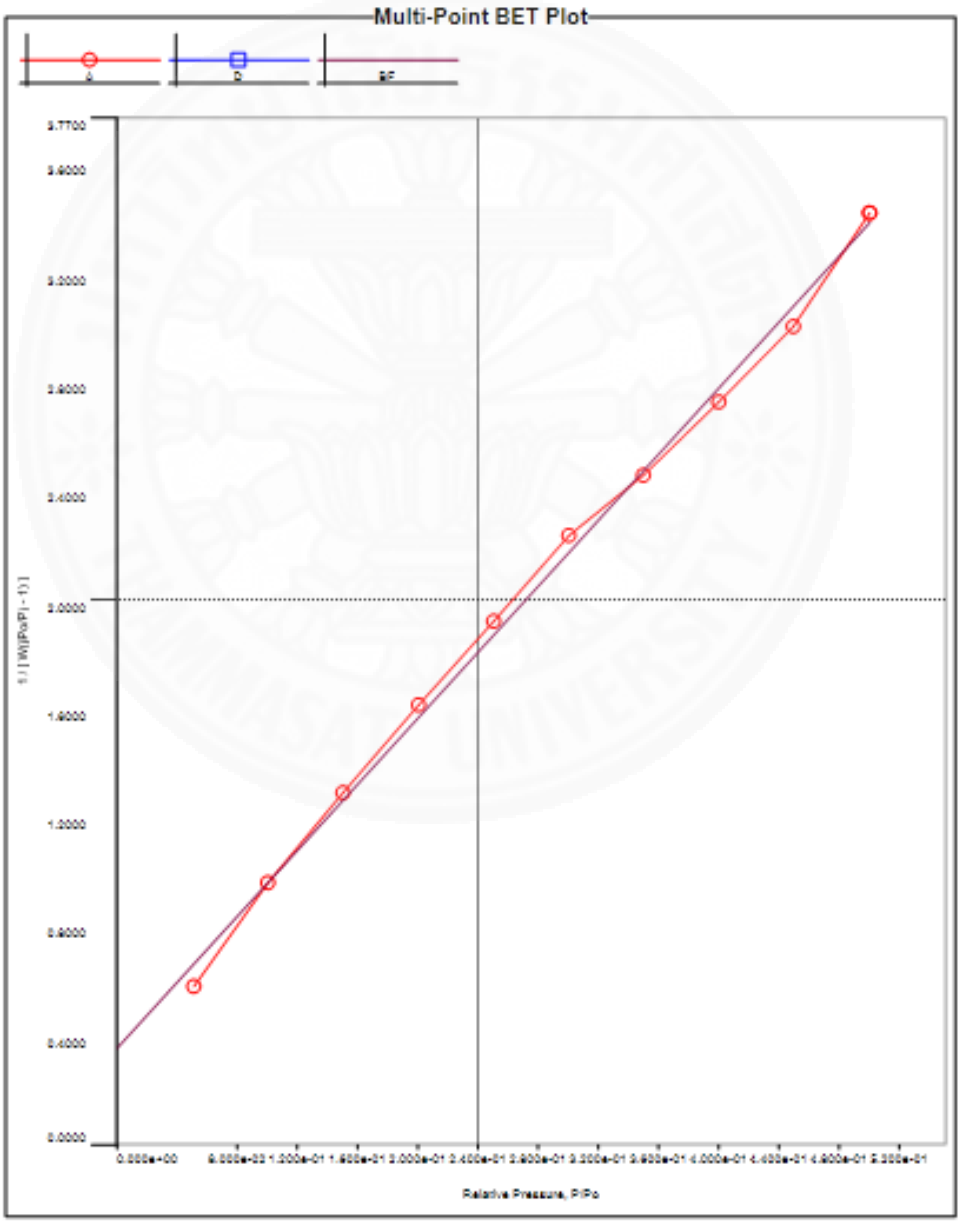

Figure 4.40 BET-plot of mGO.

Ref. code: 25595722040614EIP

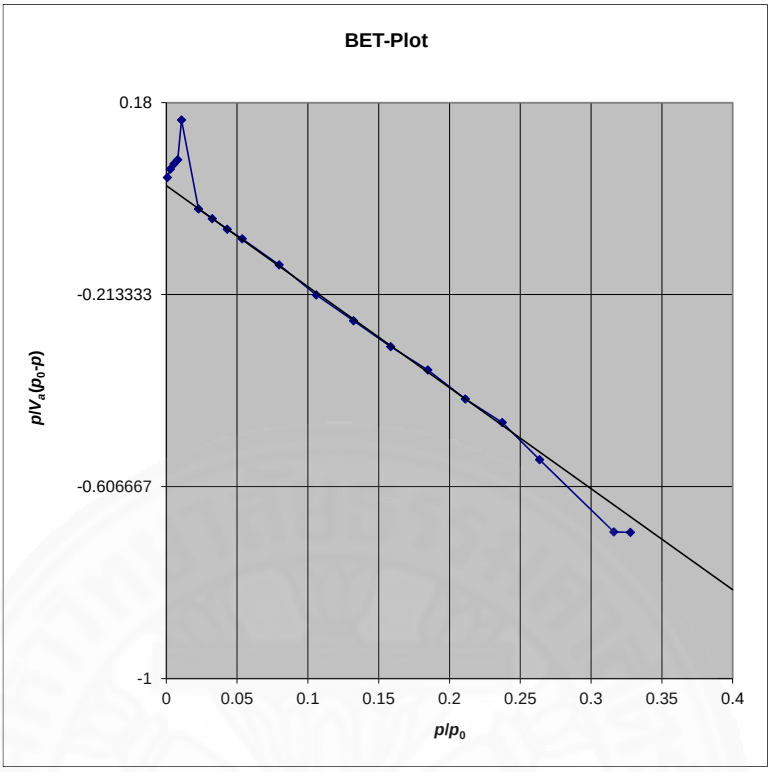

Figure 4.41 BET-plot of filter paper.

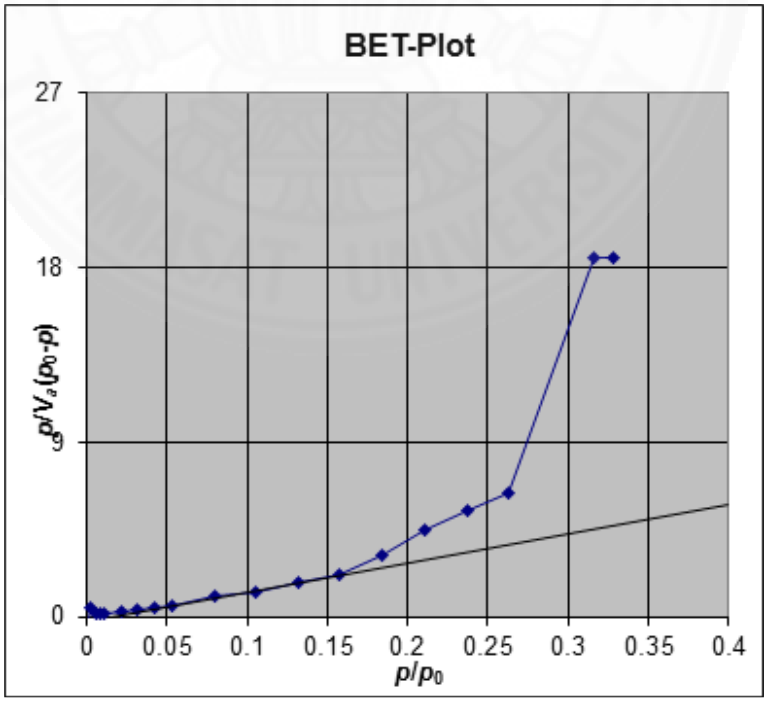

Figure 4.42 BET-plot of reed diffuser.

Ref. code: 25595722040614EIP

Chapter 5

Conclusions and Recommendations

Microwave graphene oxide or reduced graphene oxide can be synthesized from graphene oxide using microwave thermal method. Microwave graphene oxide or mGO is black fluffy and light weight. In this study, mGO was used as a sorbent to control release of some aroma compounds such as menthol, thymol, citronellol, and geraniol.

The appearance of menthol-loaded mGO in the low ratio of 1:1 (mGO:menthol) is homogeneous but the menthol-loaded mGO in the higer ratio than 1:1 started to show the crystal of menthol indicating incomplete miscibility at high loading. mGO can load menthol completely at about 1 times of its weight. While filter paper-loaded menthol and reed diffuser-loaded menthol appear to be heterogeneous even in lowest ratio of 1:0.5, they can load menthol lower than 1 times of its weight. For other aroma compounds such as thymol, citronellol, and geraniol, they can be mixed completely with mGO even at high loading ratio of 1:2.

The overall average release rates of menthol on all types of sorbents used are slower than that of pure menthol. At the temperature of 80°C, the average release rate of menthol-loaded onto mGO was about 8 times slower than that of pure menthol and about 7 times slower compared to that of the traditional reed diffuser and filter paper. For other commonly used substrates such as filter paper and reed diffuser, they can decrease the release rate of menthol released only slightly. Therefore, mGO can be used as a novel sorbent for slow release of menthol with much better slow release performance than those of traditional cellulosic materials.

Thymol-loaded onto mGO has a slower release rate compared to that of neat thymol by about 3 times. Filter paper and reed diffuser cannot decrease the release rate of thymol. For citronellol, mGO can help slow down the average release rate of citronellol by about 4.5 times slower than that of the pure citronellol and 1.8 times slower than that of traditional reed diffuser or filter paper.

In contrast, geraniol-loaded mGO has a fastest release rate compared to that of pure geraniol and other sorbents. mGO cannot slow down the release rate of geraniol but it even accelerates the release rate of geraniol by about 2.7 times. While filter paper and reed diffuser can slow down the release rate of geraniol by about 2.4 times.

Loading efficiency of mGO is around 80-93% for menthol, thymol, and citronellol but the mGO has only 55-68% loading efficiency for geraniol. For filter paper and reed diffuser is around 90%, and 80%, respectively, for all aroma compounds used which were menthol, thymol, citronellol, and geraniol. mGO cannot load geraniol as well as filter paper and reed diffuser.

The structures and functional groups of the samples from FTIR and ^{1}H-NMR results indicate that menthol are strongly adsorbed onto mGO and has reduced its

Ref. code: 25595722040614EIP

releasing rate significantly which is not seen in the reed diffuser and filter paper. The result that is also in the same trend as that of the menthol release rate observed in the TGA results. There may be chemical changes in the structure of menthol due to oxidization of menthol by mGO, however, the scent seems not to change. For thymol and citronellol on all sorbents, there are no significant change in chemical structures, they probably have only been physically adsorbed onto the sorbent.

On the contrary, geraniol is strongly adsorbed onto filter paper and reed diffuser more than mGO. The structure of geraniol was changed by oxidation of mGO causing compounds which have faster release rate. For geraniol loaded onto filter papers and reed diffuser, there seems to be no significant chemical change that can be observed from their FTIR or NMR spectra. The geraniol release rate is also slow down a little bit due probably to physisorption onto these sorbents.

Ref. code: 25595722040614EIP

References

1. Adorjan B, Buchbauer G. Biological properties of essential oils: an updated review. Flavour and Fragrance Journal. 2010;25(6):407-26.
2. Zhu Y, Murali S, Stoller MD, Velamakanni A, Piner RD, Ruoff RS. Microwave assisted exfoliation and reduction of graphite oxide for ultracapacitors. Carbon. 2010;48(7):2118-22.
3. Edris AE. Pharmaceutical and therapeutic Potentials of essential oils and their individual volatile constituents: a review. Phytotherapy Research. 2007;21(4):308-23.
4. Information NCfB. PubChem Compound Database; CID=16666 [cited 2016 May 11]. Available from: https://pubchem.ncbi.nlm.nih.gov/compound/16666.
5. CSID. L-(-)-Menthol. Available from: http://www.chemspider.com/Chemical-Structure.15803.html.
6. Zhang J, Yu M, Yuan P, Lu G, Yu C. Controlled release of volatile (−)-menthol in nanoporous silica materials. Journal of Inclusion Phenomena and Macrocyclic Chemistry. 2011;71(3):593-602.
7. Herman A, Herman AP. Essential oils and their constituents as skin penetration enhancer for transdermal drug delivery: a review. Journal of Pharmacy and Pharmacology. 2015;67(4):473-85.
8. Anthony KP, Deolu-Sobogun SA, Saleh MA. Comprehensive Assessment of Antioxidant Activity of Essential Oils. Journal of Food Science. 2012;77(8):C839-C43.
9. Astani A, Reichling J, Schnitzler P. Comparative study on the antiviral activity of selected monoterpenes derived from essential oils. Phytotherapy Research. 2010;24(5):673-9.
10. Lang G, Buchbauer G. A review on recent research results (2008–2010) on essential oils as antimicrobials and antifungals. A review. Flavour and Fragrance Journal. 2012;27(1):13-39.
11. Kuorwel KK, Cran MJ, Sonneveld K, Miltz J, Bigger SW. Essential Oils and Their Principal Constituents as Antimicrobial Agents for Synthetic Packaging Films. Journal of Food Science. 2011;76(9):R164-R77.
12. Wu Y, Qin Y, Yuan M, Li L, Chen H, Cao J, et al. Characterization of an antimicrobial poly(lactic acid) film prepared with poly(ε-caprolactone) and thymol for active packaging. Polymers for Advanced Technologies. 2014;25(9):948-54.
13. de Souza EL, da Cruz Almeida ET, de Sousa Guedes JP. The Potential of the Incorporation of Essential Oils and Their Individual Constituents to Improve Microbial Safety in Juices: A Review. Comprehensive Reviews in Food Science and Food Safety. 2016;15(4):753-72.
14. CSID. Thymol. Available from: http://www.chemspider.com/Chemical-Structure.21105998.html
15. Information. NCfB. PubChem Compound Database; CID=8842 [cited 2016 May 11]. Available from: https://pubchem.ncbi.nlm.nih.gov/compound/8842.
16. Voon HC, Bhat R, Rusul G. Flower Extracts and Their Essential Oils as Potential Antimicrobial Agents for Food Uses and Pharmaceutical Applications. Comprehensive Reviews in Food Science and Food Safety. 2012;11(1):34-55.
17. CSID. Citronellol. Available from: http://www.chemspider.com/Chemical-Structure.13850135.html.

Ref. code: 25595722040614EIP

18. Information NCfB. PubChem Compound Database; CID=637566. Available from: https://pubchem.ncbi.nlm.nih.gov/compound/637566
19. CSID. Geraniol. Available from: http://www.chemspider.com/Chemical-Structure.13849989.html.
20. Ming Dong XY, Li YY, Wei F, Zhou Y, Zhou SL, Zhu JH. Novel menthol releaser derived from as-synthesized mesoporous silica. RSC Advances. 2015;5(8):5494-500.
21. Zhu L, Lan H, He B, Hong W, Li J. Encapsulation of Menthol in Beeswax by a Supercritical Fluid Technique. International Journal of Chemical Engineering. 2010;2010:7.
22. Todorova SB, Silva CJSM, Simeonov NP, Cavaco-Paulo A. Cotton fabric: A natural matrix suitable for controlled release systems. Enzyme and Microbial Technology. 2007;40(7):1646-50.
23. Tekin R, Bac N, Warzywoda J, Sacco Jr A. Encapsulation of a fragrance molecule in zeolite X. Microporous and Mesoporous Materials. 2015;215:51-7.
24. Bosch-Navarro C, Coronado E, Marti-Gastaldo C, Sanchez-Royo JF, Gomez MG. Influence of the pH on the synthesis of reduced graphene oxide under hydrothermal conditions. Nanoscale. 2012;4(13):3977-82.
25. Dreyer DR, Park S, Bielawski CW, Ruoff RS. The chemistry of graphene oxide. Chemical Society Reviews. 2010;39(1):228-40.
26. Hummers WS, Offeman RE. Preparation of Graphitic Oxide. Journal of the American Chemical Society. 1958;80(6):1339-.
27. Pei S, Cheng H-M. The reduction of graphene oxide. Carbon. 2012;50(9):3210-28.
28. analysis Lomcac. Graphenes. Available from: https://www.utu.fi/en/units/sci/units/chemistry/research/mcca/Pages/Sub-pages%20of%20Functional%20Materials/Graphenes.aspx.
29. Wei T, Fan Z, Luo G, Zheng C, Xie D. A rapid and efficient method to prepare exfoliated graphite by microwave irradiation. Carbon. 2009;47(1):337-9.
30. Sigma-Aldrich. Reduced graphene oxide. Available from: http://www.sigmaaldrich.com/catalog/product/aldrich/777684?lang=en&region=TH.
31. Pisklak TJ. Fragrance dispensing wick and method. Google Patents; 2010.
32. Herd TP, Rouchou V. Liquid composition for air freshener systems. Google Patents; 2011.
33. Rosener MJ, Blaylock RD, Van Epps DL. Releasing fragrances into the air. Google Patents; 2010.
34. Motylinski N, Mehfar AA. Spill-proof aerator for low volatile compound solutions. Google Patents; 2012.
35. Decker DNM, Dodson S. Oil lamp, air freshener and/or fragrance release apparatus and wick therefor. Google Patents; 2009.
36. Chen X, Niu Z, Ma J. Method of preparing reduced graphene oxide foam. Google Patents; 2013.
37. Fashi A, Khanban F, Yaftian MR, Zamani A. The cooperative effect of reduced graphene oxide and Triton X-114 on the electromembrane microextraction efficiency of Pramipexole as a model analyte in urine samples. Talanta. 2017;162:210-7.

Ref. code: 25595722040614EIP

38. Feng C, Yi Z, She F, Gao W, Peng Z, Garvey CJ, et al. Superhydrophobic and Superoleophilic Micro-Wrinkled Reduced Graphene Oxide as a Highly Portable and Recyclable Oil Sorbent. ACS Applied Materials & Interfaces. 2016;8(15):9977-85.
39. Al-Bayati FA. Isolation and identification of antimicrobial compound from Mentha longifolia L. leaves grown wild in Iraq. Annals of Clinical Microbiology and Antimicrobials. 2009;8:20-.
40. WIKIPEDIA. Menthol. Available from: https://en.wikipedia.org/wiki/Menthol.
41. Frederick A. Bettelheim WHB, Mary K. Campbell,Shawn O. Farrell,Omar Torres. Introduction to Organic and Biochemistry. EIGHT edition ed: Mary Finch; 2013.
42. More JD, Finney NS. A Simple and Advantageous Protocol for the Oxidation of Alcohols with o-Iodoxybenzoic Acid (IBX). Organic Letters. 2002;4(17):3001-3.
43. Dapurkar SE, Kawanami H, Chatterjee M, Rode CV, Yokoyama T, Ikushima Y. Selective catalytic oxidation of geraniol to citral with molecular oxygen in supercritical carbon dioxide. Applied Catalysis A: General. 2011;394(1–2):209-14.
44. Pubchem. Citral. Available from: https://pubchem.ncbi.nlm.nih.gov/compound/Citral#section=Top.

Ref. code: 25595722040614EIP